Cytochrome P450 Reductases in Plants

Bethany Mostert[1] and Deyu Xie[2*†]

[1*]Department of Plant and Microbial Biology, North Carolina State University, 100 Derieux Pl, Raleigh, 27607, NC, United States.
[2]Department of Plant and Microbial Biology, North Carolina State University, 100 Derieux Pl, Raleigh, 27607, NC, United States.

*Corresponding author(s). E-mail(s): dxie@ncsu.edu;
Contributing authors: bhmoster@ncsu.edu;
†Bethany Mostert was the primary author of the manuscript and prepared all figures. Deyu Xie supervised the work, edited the manuscript, and provided scientific guidance throughout.

Abstract

Cytochrome P450 reductase (CPR) is a membrane anchored enzyme in the endoplasmic reticulum (ER) which shuttles electrons from NADPH to cytochrome P450 (CYP) enzymes via FAD and FMN co-factors. CPRs constitute a small protein family that include one to four members (e.g., one in humans and mammals and three in *Sorghum bicolor*). They partner with a large number of CYP proteins involved in the biosynthesis of key plant metabolites, such as CYP71AV1 involved in artemisinin biosynthesis within *Artemisia annua*. To date, although the functions of yeast, human, and mammal CPRs have been comprehensively characterised, their functions among plant homologues remain more understudied. The findings presented here are integrated with published data to provide an updated overview of the plant CPR gene family, focusing on their evolution, preferences in plant primary and secondary metabolism, the functional contributions of their various domains, and the influence of the connecting domain and hinge on conformational dynamics. Although CPR1 and CPR2 have been reported to involve plant primary and secondary metabolism, the phylogenetic analyses presented here suggest that the current classification of some CPR members requires re-evaluation to better resolve their evolutionary relationships and functional divergence. The length and amino acid composition of the hinge and its contributions to conformational flexibility are also discussed. Available evidence indicates that the structural properties of the CPR hinge is a critical determinant of CPR conformational ability, thus influencing the efficiency of electron transfer to CYP

enzymes. In summary, this updated synthesis provides new insights into the evolution, structure, and functional diversification of plant CPRs and establishes a framework for elucidating their roles in plant metabolism.

Keywords: cytochrome P450, cytochrome P450 reductase, metabolism, protein-protein interactions, protein evolution, protein structure

1 Introduction

Plants are rich sources of metabolites, many of which are fundamental to human health (Cheng et al., 2023; McClune et al., 2025; Miller, Hollatz, & Schuler, 2021; Parage et al., 2016; Tiedge, Roda, Smith, & Moghe, 2025; Xie, Ma, Judd, & Jones, 2016). These specialised metabolites play vital roles in plant reproduction and adaptation (e.g. attraction of pollinators, defense against predators, and resistance to abiotic stresses such as high UV radiation and drought) (Hamberger & Bak, 2013; Tiedge et al., 2025). Given their importance, metabolic engineering of these plant compounds has been extensively explored in a number of native and heterologous hosts (Brown, Clastre, Courdavault, & O'Connor, 2015; R. Chen et al., 2022; Jennewein et al., 2005; Paddon & Keasling, 2014; Ro et al., 2008; Spivak et al., 2009; Van Den Brink, Van Zeijl, Brons, Van Den Hondel, & Van Gorcom, 1995; Walters Biggs et al., 2016). Consequently, numerous enzyme families, including cytochrome P450 (CYP) monooxygenase and cytochrome P450 reductase (CPR), have been identified to catalyse various steps within plant biosynthetic pathways (Z. Chang et al., 2018; X. Chen et al., 2014; Choi et al., 2023; Gu et al., 2019; Hansen et al., 2018; Karunanithi et al., 2019; Khanom, Jang, & Lee, 2019; Knosp et al., 2024; Krishnamurthy, Vishal, Bhal, & Kumar, 2021; X. Lu et al., 2013; Mao, Seebeck, Schrenker, & Yu, 2013; Neunzig et al., 2013; Pastorczyk et al., 2020; Sagwan-Barkdoll & Anterola, 2018; Sintupachee, Promden, Ngamrojanavanich, Sitthithaworn, & De-Eknamkul, 2015; Teoh, Polichuk, Reed, Nowak, & Covello, 2006; Urban, Mignotte, Delorme, & Pompon, 1997).

CYP enzymes comprise a superfamily involved in the oxygenation of various metabolites (Hamberger & Bak, 2013; Nelson & Werck-Reichhart, 2011; Werck-Reichhart, Nelson, & Renault, 2024). The expansion and neofunctionalisation of this family throughout plant evolution has played a key role in diversifying the structures of plant metabolites (Hamberger & Bak, 2013; Nelson & Werck-Reichhart, 2011). Another defining characteristic of many CYPs is their close interaction with associated reductase enzymes. For example, Class II CYPs from eukaryotes are membrane anchored in the ER and characterised to be primarily functional via two-electron reduction by a redox partner such as cytochrome P450 reductase (CPR), and cytochrome b_5 (CYB5) (which also functions as a CPR electron acceptor) (Ershov et al., 2019; Iyanagi, Xia, & Kim, 2012; Warman et al., 2005).

CPRs are a small enzyme family with essential roles in all organisms. CPRs bind the flavin molecules flavin adenine dinucleotide (FAD) and flavin mononucleotide (FMN) and are thus related to other flavin containing proteins present across all taxa

(K. Jensen & Møller, 2010; Porter & Kasper, 1985). The basic similarities and architectural differences among diflavin reductases have been well summarised (Aigrain, Fatemi, Frances, Lescop, & Truan, 2012; Iyanagi et al., 2012; Murataliev, Feyereisen, & Walker, 2004). Based on their sequence similarity, CPRs and other diflavin enzymes are predicted to be the result of an ancestral fusion between an FMN containing bacterial flavodoxin and FAD containing ferredoxin-$NADP^+$ reductase (FNR) (Iyanagi et al., 2012; Porter & Kasper, 1985). To date, three types of microbial diflavin enzymes have been identified, including sulphite reductase (SiR) (Tavolieri et al., 2019) (found also in some plants) (Kim, Nakayama, Toyota, Kurisu, & Hase, 2016), flavocytochrome P450 BM3 (Warman et al., 2005), and a recent diflavin nitrate reductase (NasN) from *Mycolicibacterium smegmatis* (refer Fig. 1) (Tan et al., 2020). In higher level organisms, diflavin enzymes include methionine synthase reductase (MSR) and novel reductase 1 (NR1), as well as endothelial, neuronal, and inducible nitric oxide synthases (eNOS, nNOS, iNOS) (refer Fig. 1) (Haque et al., 2014; K. Jensen & Møller, 2010; Nair & Crane, 2026).

Due to their shared ancestry, diflavins possess conserved aromatic residues, which lie planar to the isoalloxazine rings of FAD and FMN that are involved in electron flux (refer Fig. 2) (Meints, Simtchouk, & Wolthers, 2013; Porter & Kasper, 1985; Whitelaw, Tonkin, Meints, & Wolthers, 2015). In particular, FAD is gated by a C-terminal tryptophan that displaces NADPH and $NADP^+$ (refer Fig. 2, refer Fig. 3) (Whitelaw et al., 2015). This effectively divides the steps of electron transfer (ET) from NADPH to FAD and then from $FADH_2$ to FMN (refer Fig. 3) (Musumeci, Botti, Buschiazzo, & Ceccarelli, 2011; Whitelaw et al., 2015).

The catalytic activity of numerous diflavin enzymes are predominantly NADPH-dependent, which is consistent with their FNR evolutionary origins. NADPH preference is largely attributed to binding of the 2′-phosphate of the adenosine moiety (2′-P-AMP) due to interactions with conserved arginine residues found throughout microsomal FNR-type enzymes (Deng et al., 1999; Monchietti, Rivero, Ceccarelli, & Catalano-Dupuy, 2021). While human MSR varies in amino acid composition at the NADPH binding site, its catalytic preference for NADPH remains (Wolthers, Lou, Toogood, Leys, & Scrutton, 2007). Thus, incorporation of FNR-derived sequences concomitantly conserves a binding and catalytic preference for NADPH. This biochemical feature was further substantiated by a NasN (refer Fig. 1) identified from *M. smegmatis* (Tan et al., 2020).

Whereas most nitrate reductases from related and phylogenetically distant species utilise NADH and contain either ferredoxin or single-flavin domains, NasN, which harbours a diflavin architecture, exhibits a greater catalytic preference for NADPH than NADH (Tan et al., 2020). Additionally, compared with non *NasN* bacterial species, *NasN*-expressing *M. smegmatis* possessed a higher oxygen tolerance and a higher growth rate under aerobic conditions. These advantages allowed *M. smegmatis* to survive better than other microbes in nitrate-limited conditions (Tan et al., 2020). Such outcomes likely resulted from the increased ET efficiency of the diflavin architecture. This is because swift ET is facilitated by the presence of a connecting domain and flexible hinge that tether the respective FMN and FAD binding regions close to each other (refer Fig. 1) (Aigrain, Pompon, Moréra, & Truan, 2009; Iyanagi et al., 2012; Lamb

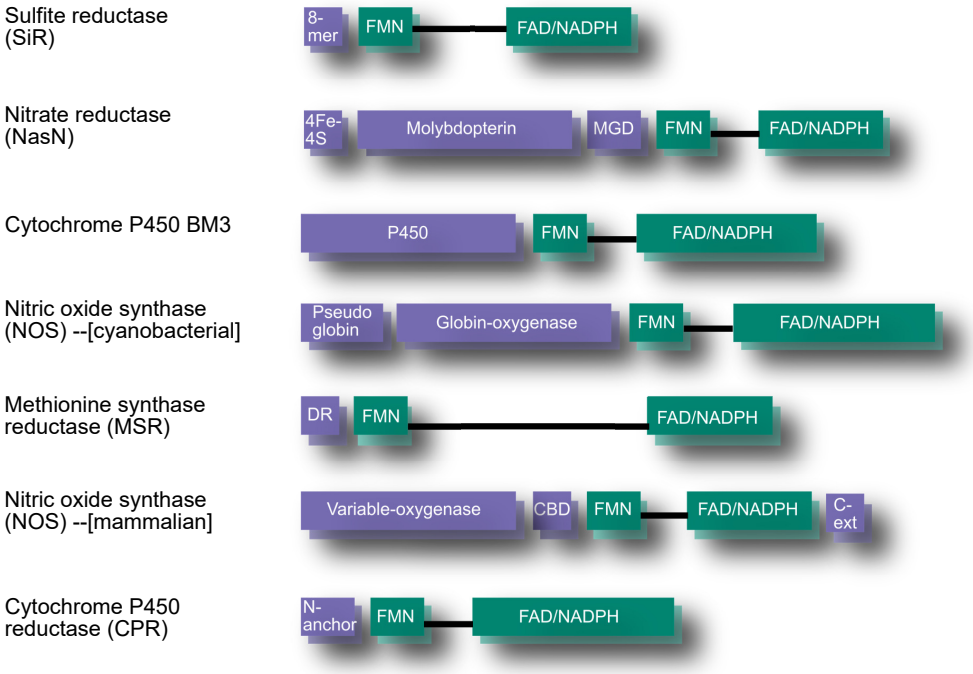

Fig. 1 Summary of representative diflavin enzymes. Enzymes are ordered based on species descent, not enzyme relatedness. SiR, NasN, P450 BM3, and the first NOS are all bacterial derived examples, while MSR, NOS, and CPR are mammalian based. The CPR basic architecture is shared in plants. Non-diflavin architectural units are coloured in purple and diflavin units are coloured in teal. Black lines denote hinges and are exaggerated to highlight length as a distinguishing feature among the SiR and MSR enzymes. Abbreviations: FMN = flavin mononucleotide binding domain, FAD = flavin adenine dinucleotide binding domain, NADPH = NADPH binding domain, MGD = molybdopterin guanine dinucleotide, DR = disordered region, CBD = calmodulin binding domain, C-ext = C-terminal extension.

et al., 2006; Waskell & Kim, 2015). This moves the protein domains (e.g., NADPH/-FAD and FMN binding domains) in a controlled manner to facilitate inter-domain and inter-protein ET via transitions from closed to open conformational states (Iyanagi et al., 2012).

A typical hinge/flexible linker among the diflavins is 12-15 amino acids long, but MSR, and more recently, a bacterial SiR protein have been found with hinges up to 80 and 30 amino acids long, respectively (refer Fig. 1) (Aigrain et al., 2009; Haque et al., 2014; Tavolieri et al., 2019; Wolthers et al., 2007). It is possible that these longer hinges are required to accommodate the large, unique complexes that MSR and SiR form with their respective oligomeric subunits: methionine synthase and sulphite reductase flavoprotein (Tavolieri et al., 2019). For instance, a recent multimeric model of *E. coli* SiR has proposed that its longer hinge facilitates highly variable protein conformations, allowing for ET between multiple SiR proteins (Tavolieri et al., 2019). Elucidation of crystal contacts led to a model of ET from NADPH to the FAD of SiR1 and to the FMN

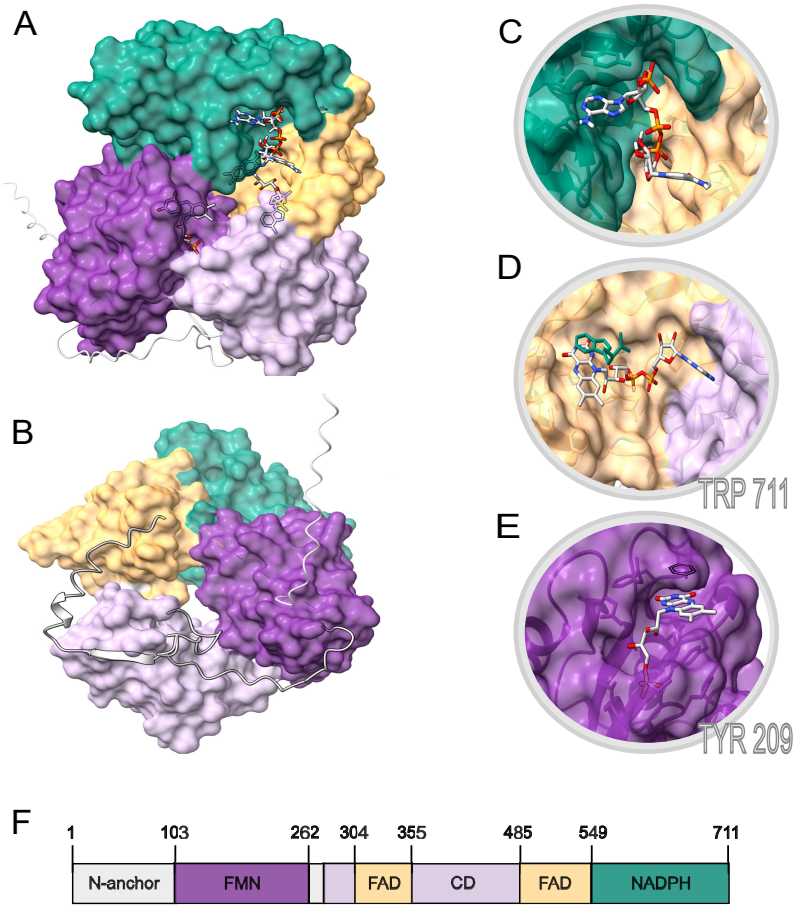

Fig. 2 Surface structure of ATR2, *A. thaliana* (5GXU). Missing residues 1–103 (N-terminal anchor), 262–304 (hinge + connecting domain), and 380–397 (connecting domain) were predicted via ColabFold and integrated to the 5GXU crystal structure in ChimeraX through homology modelling. Grey: N-terminal anchor and missing hinge/connecting domain residues. Dark purple: FMN binding domain. Light purple: connecting domain. Yellow: FAD binding domain. Teal: NADPH binding domain. (A) Complete ATR2 structure with cofactor-bound side facing out. (B) Complete ATR2 structure with hinge side facing out. Residues 262–304 (hinge + connecting domain) are pictured as grey loops. (C) Binding mode for NADPH. (D) Binding mode for FAD. The interfacing and conserved C-terminal tryptophan from the NADPH domain (711) is in teal. (E) Binding mode for FMN. The interfacing and conserved tyrosine (209) is situated above the isoalloxazine ring. (F) A linear diagram showing domain arrangement corresponds to the domain colours in the protein models. The numbers above indicate approximate amino acid positions of each domain. While the connecting domain and FAD domain are intertwined in linear sequence, each forms a discrete domain in the protein structure.

of SiR2 which reduces the associated terminal protein acceptor (Tavolieri et al., 2019). Structural modelling and biochemical analysis of MSR has led to a similar, albeit less defined, interaction mechanism for its longer hinge (Bassila et al., 2017; Haque et al., 2014; Wolthers et al., 2007). Like *E. coli* SiR, MSR possesses an extended open conformation (Haque et al., 2014; Tavolieri et al., 2019). Additionally, its propensity

to dimerise and participate in a tightly integrated multi-protein metabolon, suggests that MSR may also pass electrons between the domains of more than one protein (Bassila et al., 2017; Wolthers et al., 2007).

The connecting domain, which follows the hinge, is an important structure next to the FAD-binding region. This domain arises as an insertion within the FNR-like module. Its presence results in an interruption of the FAD binding domain sequence, which is a feature conserved across diflavin reductases, with modest variation in length among family members (refer Fig. 2) (Iyanagi et al., 2012; Niu et al., 2017; Tavolieri et al., 2019; Wolthers et al., 2007). Despite this apparent discontinuity in sequence, structural studies of CPR show that the connecting domain and FAD-binding domain fold into distinct, well-defined units (refer Fig. 2). Functionally, the connecting domain contributes to the spatial organisation of the FMN and FAD cofactors and plays an important role in optimal alignment of the two domains and FMN's conformational changes (Aigrain et al., 2012; Laursen, Jensen, & Møller, 2011; Porter & Kasper, 1985).

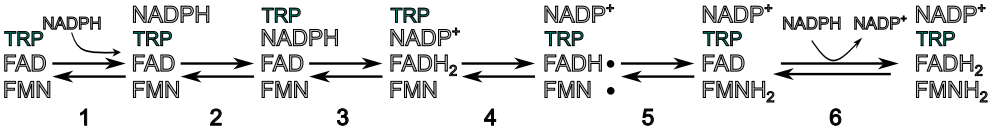

Fig. 3 Electron transfer steps in CPR, adapted from (Whitelaw et al., 2015). TRP represents TRP711. Step 1: NADPH binds to fully oxidised CPR. Step 2: TRP is displaced by NADPH. Step 3: The first hydride transfer occurs and NADPH is oxidised to $NADP^+$ and FAD is reduced to $FADH_2$. Step 4: First single ET from FAD to FMN (formation of the FADH and FMN semiquinones). TRP displaces $NADP^+$. Step 5: Second single ET from FADH to FMN. Step 6: Another molecule of NADPH is added for complete enzymatic reduction. This step includes steps 1–3 for formation of the $FADH_2$ hydroquinone.

Of all the diflavin enzymes investigated, CPR is the only one with an N-terminal anchor (refer Fig. 1) (Aigrain et al., 2012). This structure hydrophobically embeds CPR within the ER and ensures its interactions with the catalytic domain of CYPs at the ER surface (Aigrain et al., 2012).

Despite all their shared features, previous research has reported that differences in diflavin structure and molecular binding domains changes their biophysical and biochemical activities. Haque et al. (2014) compared the rates of conformational switching with the ET capacities of four human diflavin enzymes: CPR, MSR, neuronal nitric oxide synthase (nNOS), and endothelial nitric oxide synthase (eNOS). In their experiments, the enzymes were completely reduced with NADPH in a cytochrome *c* saturated reaction to estimate ET flow kinetics (Haque et al., 2014). The results that followed were used to characterise the proportion of open and closed conformations for each reductase. This study showed that, in spite of slower ET from FAD to FMN for CPR (e.g., steps 4-6, refer Fig. 3), its fast conformational switching compensated for its overall electron flux rate (Haque et al., 2014). Conversely, MSR, nNOS, and eNOS could not compensate for slower electron flux due to their slower conformational switching (Haque et al., 2014). This study revealed that CPR possesses the quickest ET flux rate of the investigated human diflavin enzymes (Haque et al., 2014).

Further mechanistic investigations have proposed that the efficient ET in CPR likely results from increased hydrogen bonds and salt bridges, high surface area for interfacing residues, and dynamic hinge motions (Campelo et al., 2017; Haque et al., 2014; Niu et al., 2017; S. Xia & Hirao, 2025; B. Zhang et al., 2022).

2 Genomic and Stoichiometric Balancing of CPR in Plant and Animal CYP Systems

Though the prevailing mechanism of CPR on CYP reduction is shared among animals, plants, and fungi due to the conservation of the NAD, FAD, and FMN binding domains, ongoing research shows that CPR homologues differ genomically, transcriptionally, and metabolically (Benveniste, Lesot, Hasenfratz, Kochs, & Durst, 1991), (Lah et al., 2011; Lesot, Benveniste, Hasenfratz, & Durst, 1990; Ohta & Mizutani, 2004; Parage et al., 2016; Ro, Ehlting, & Douglas, 2002; Su et al., 2017; Whitelaw et al., 2015). To date, CPR has been characterised to consist of a small family, with one member in mammals and humans (Porter, Beck, & Kasper, 1990; Simmons, Lalley, & Kasper, 1965) and 2 to 4 members in plants and some fungi (Benveniste et al., 1991; Lah et al., 2011; Su et al., 2017; Urban et al., 1997; B. Zhang et al., 2022). Since the discovery of multiple CPRs in plants and fungi, functional characterisation has placed them into two subclasses—one involved in primary metabolism (CPR1) and the other involved in secondary metabolism (CPR2) (Ohta & Mizutani, 2004; Ro et al., 2002; Urban et al., 1997).

In an expanded CPR phylogeny of 98 sequences, CPR1 and CPR2 form the largest clades (refer Fig. 4). Within this larger phylogeny, previously annotated CPR1 proteins group into the CPR2 clade (e.g., *Tripterygium wilfordii* CPR1, *Artemisia annua* CPR1, and *Aconitum vilmorinianum* CPR1) (refer Fig. 4). Meanwhile, other annotated proteins such as *Petroselinum crispum* CPR2a, *Tripterygium wilfordii* CPR3, and *Tripterygium wilfordii* CPR4 group into the CPR1 clade (refer Fig. 4). This demonstrates a greater need for characterisation of these closely related CPRs. Consequently, these CPRs likely possess uncharacterised functions in plant primary or secondary metabolism.

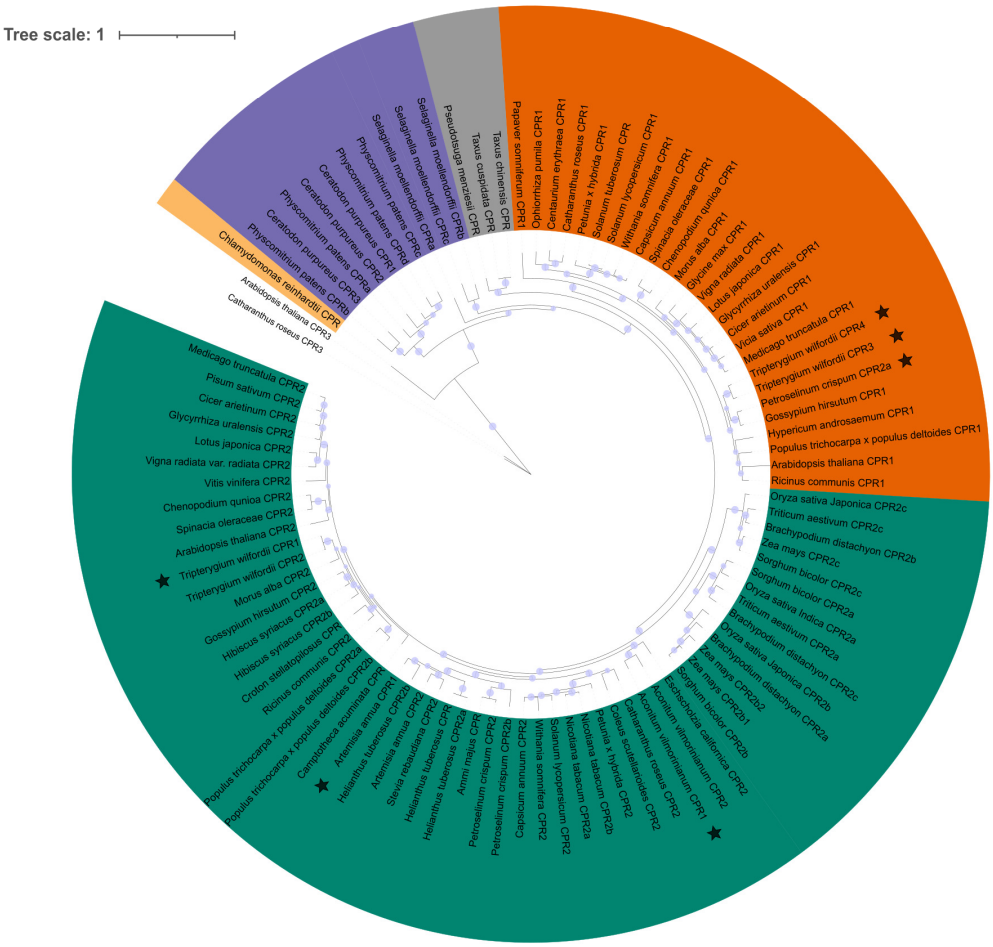

Fig. 4 Predicted secondary structure of CPR N-terminal anchors across species. CPRs are arranged according to phylogenetic relationships based on the CPR protein sequences rather than organismal phylogeny. N-terminal anchor lengths were inferred from AlphaFold3 predictions, while the presence and approximate boundaries of α-helical segments were independently predicted using AlphaFold3 and JPred. Only residues predicted to form α-helices are shown (blue helices), and the boundaries between disordered and helical regions are indicated by residue numbers. Human CPR was included as a benchmark because the N-terminal anchor has been experimentally observed by (Barnaba, Martinez, Taylor, Barden, & Brozik, 2017); both AlphaFold3 and JPred predicted the experimentally reported helix boundaries within approximately ± 2 residues. AlphaFold3 predicted high confidence for most helical regions (pLDDT > 90), with lower confidence observed for *S. cerevisiae* (yeast) and *Taxus cuspidata* (Japanese yew). Predicted helix presence and overall architecture are considered more reliable than the precise boundaries of individual helices.

One proposed explanation for the duplication of *CPR* genes in plants is that the expansion of the *CYP* family required more CPRs to meet ET needs (Choi et al., 2023). For example, the human genome has 57 *CYP*s and 1 *CPR*, while the *Arabidopsis thaliana* genome includes 246 *CYP*s and two *CPR*s (**??**). Likewise, other plant

species have more *CYP*s than humans and mammals (**??**). These differences likely result from the lack of complicated mammalian metabolism compared to the expansive secondary metabolisms in *A. thaliana* and other plants. These data form a fundamental hypothesis that the specific ratios between *CYP*s and *CPR* in plants, animals, and microbes might be associated with the degree of metabolic complexity found within each organism. Interestingly, the genome of *Physcomitrium patens*, a moss species, is estimated to have 98 potential *CYP*s and four *CPR* paralogues (K. Jensen & Møller, 2010) (Table 1). Though the number of *CYP*s is lower in this species, the presence of four *CPR*s may help to expand the metabolism of *P. patens* in ways that have yet to be explored. This hypothesis is based on CPR biased metabolism, a concept put forward by Jensen et al. (2021) to describe how CPR paralogues can differentially partner with CYPs to potentially favour or disfavour metabolic outcomes.

Table 1: Phylogenetic comparison of cytochrome P450 (CYP) and cytochrome P450 reductase (CPR) copy numbers across representative taxa. The genes reported here are representative of copy number, but may not be reflective of gene expression, nor the functional reality of the CYP counts. Furthermore, different publications use different metrics for reporting—listing CYPs at either the genome or transcript level can result in different copy numbers.

Organism	**Common Name**	**Taxa**	**CYP**	**CPR**	**CPRs characterised**
Homo sapiens	human	Mammalia	47	1	CPR
Rattus norvegicus	rat	Mammalia	89	1	CPR
Phanerochaete chrysosporium	white rot fungus	Fungi	123	1	CPR
Botryococcus braunii	green algae	Chlorophyta	36	1	CPR
Chlamydomonas reinhardtii	green algae	Chlorophyta	39	4	-
Physcomitrium patens	spreading earth moss	Embryophyta	98	4	-
Selaginella moellendorffii	Moellendorf's spikemoss	Tracheophyta	390	3	-
Taxus chinensis	Chinese yew	Gymnosperm	118	1	-
Taxus cuspidata	Japanese yew	Gymnosperm	193	1	CPR
Oryza sativa	rice	Monocot	334	3	CPR1, CPR2, CPR3
Sorghum bicolor	sorghum	Monocot	372	3	CPR2a, CPR2b, CPR2c
Zea mays	corn	Monocot	318	3	-
Eschscholzia californica var. Aurantiaca Orange King	California poppy	Eudicot (basal)	189	2	CPR
Vitis vinifera	grapevine	Eudicot (rosid)	235	2	-

Table 1: (continued)

Organism	Common Name	Taxa	CYP	CPR	CPRs characterised
Arabidopsis thaliana	thale cress	Eudicot (rosid)	273	2	CPR1, CPR2
Populus trichocharpa x Populus deltoides	black/eastern cottonwood	Eudicot (rosid)	313	3	CPR1, CPR2, CPR3
Ricinus communis	castor bean	Eudicot (rosid)	207	2	-
Gossypium hirsutum	upland cotton	Eudicot (rosid)	366	2	CPR1, CPR2
Citrus x sinensis	navel orange	Eudicot (rosid)	153	2	-
Morus alba	mulberry	Eudicot (rosid)	174	2	CPR1, CPR2
Tripterygium wilfordii	thunder god vine	Eudicot (rosid)	1228	4	CPR1, CPR2, CPR3, CPR4
Lotus japonicus	Japanese lotus	Eudicot (rosid)	172	2	CPR1, CPR2
Solanum lycopersicum	tomato	Eudicot (asterid)	222	2	CPR1, CPR2
Catharanthus roseus	Madagascar periwinkle	Eudicot (asterid)	191	2	CPR1, CPR2, (CPR3)
Camptotheca acuminata	happy tree	Eudicot (asterid)	416	2	CPR1, CPR2

Though the functional purposes for the genomic ratio of*CYP*s to *CPR*s in plants remain to be characterised, progress has been made in describing the stoichiometry of these two enzyme families. In general, the stoichiometry of the CPR and CYP in a catalytic system needs one NADPH (two electrons), one substrate, and one O_2 to form one molecule of oxidised substrate and one H_2O (Grinkova, Denisov, McLean, & Sligar, 2012). Although the stoichiometric relevance between CPR and CYPs in the same cells remain open for detailed investigations, mammalian experimentation has revealed ratios between CPR and CYP as 1:15 (Shephard, Phillips, Bayney, Pike, & Rabin, 1983) and, in some cases, as 1:100 (Guengerich, 2002). These ratios suggest that CPR likely plays a central role in regulating ET to multiple CYPs in the same cell. Although the stoichiometry of 2-3 CPRs to CYPs has not yet been characterised in plants, based on these data, it is possible that similar stoichiometries of CPRs and CYPs might occur in plants. CPRs must therefore organise efficiently to steadily supply electrons to the large number of CYPs that compete for an interaction (Esteves et al., 2020; K. Jensen & Møller, 2010; Ralston & Yu, 2006; Shephard et al., 1983).

To date, a metabolon model has been proposed to address these observations, wherein CPRs and CYPs organise into an associated protein complex on the cytosolic surface of the ER membrane (Laursen, Møller, & Bassard, 2015; Ralston & Yu, 2006). The dhurrin metabolon was first offered as supportive evidence for this model

when all of the essential enzymes involved in dhurrin biosynthesis were co-purified from the microsomes of etiolated sorghum seedlings (Laursen et al., 2016). In addition to known pathway enzymes like CYP79A1, CYP71E1, UDP-glucosyltransferase (UGT85B1), and dhurrinase, the three CPR paralogues (SbCPR2a-c) and other reductases, cytochrome b_5 (CYB5) and CYB5 reductase (CBR) were also found enriched in the microsomal membranes (Laursen et al., 2016). Förster resonance energy transfer (FRET) analysis validated the close proximity of CYP79A1, CYP71E1, UGT85B1 and CPR2b at the ER *in-planta*, demonstrating that a complex of the two CYPs actively recruits UGT85B1 for dhurrin biosynthesis (Laursen et al., 2016).

Affinity purification, yeast-2-hybrid assays, and docking studies have also shown the involvement of potential CYP metabolons in rice, bean and snapdragon flavonoid metabolism (Nakayama, Takahashi, & Waki, 2019; Ruan et al., 2024; Y. Zhang & Fernie, 2021). Furthermore, yeast-2-hybrid and split luciferase assays were reported to identify a cytochrome b_5 isoform (CsCB5c) in a flavonoid metabolon model in tea plants, in which CsCB5c interacts with CYPs (Ruan et al., 2024). Although there is a lack of conclusive evidence regarding the differentiating roles of 2-4 CPRs in CYP associated redox reactions, these findings provide unique insight into the stoichiometric imbalances proposed for plant CPRs and CYPs (Guengerich, 2002; Manoj, Gade, & Mathew, 2010; Walters Biggs et al., 2016; H. Zhang, Im, & Waskell, 2007). Consequently, resolving the spatial and functional organisation of multiple CPRs within metabolons would substantially improve understanding for their cooperation, competition, and functional specialisation within plants.

3 Divergent Features of Plant CPR Paralogues

To date, past research has provided informative insight into the functional divergence of plant CPR homologues. Based on transcriptional and CYP co-expression data reported previously, there are two types of plant CPRs: constitutive and inducible/spatial CPRs (Lesot et al., 1990; Nicotra et al., 2010; Urban et al., 1997; X. Zhao, Zhao, Gou, & Liu, 2023). Although further investigations are necessary to comprehensively understand their functions, CPR1 is characterised to be a constitutive enzymatic CYP partner involved in plant primary metabolism, while CPR2 is considered to be inducible and spatially distinct based on its associations with plant secondary metabolism (S.B. Jensen et al., 2021; Parage et al., 2016; Ro et al., 2002; X. Zhao et al., 2023). Beyond the distinction of CPR1 and CPR2, little is known among plants possessing three or more paralogues. Two characterisation studies of a third CPR enzyme were completed in *A. thaliana* and *Catharanthus roseus* (Parage et al., 2016; Varadarajan et al., 2010). Neither ATR3 (CPR3) from *A. thaliana* nor CPR3 from *C. roseus* were able to interact with CYPs (Parage et al., 2016; Varadarajan et al., 2010). Furthermore, phylogenetic analysis places both of these enzymes into their own clade (refer Fig. 4), suggesting that these enzymes come from a distinct phylogenetic lineage that precedes the emergence of CPRs. Though both of the CPR3s had NADPH, FAD and FMN binding domains, neither possessed an N-terminal anchor and were incapable of localising to the ER; instead, they demonstrated cytosolic and nucleocytosolic localisation patterns (Parage et al., 2016; Varadarajan et al., 2010). Varadarajan et

al. (2010), deduced that ATR3 was involved in essential cellular functions such as embryogenesis. Altogether, these data support the designation of these proteins as novel reductase 1 (NR1) proteins (refer Fig. 1) (Parage et al., 2016; Varadarajan et al., 2010). Thus, these enzymes have henceforth been classed as 'false CPRs' (Varadarajan et al., 2010). Therefore, more data must follow to further characterise CPR3s to understand their function in plant metabolism and development.

Past functional analysis has observed that plant CPRs demonstrate selectivity in partnering with CYPs. While characterisation studies of plant CYPs have often relied on endogenous CPRs present in heterologous expression systems (e.g., yeast and tobacco) for their activity (Lamb et al., 2006; Laursen et al., 2016; Neunzig et al., 2013), many studies have reported that combining heterologous CYPs with yeast or tobacco CPR significantly diminishes reaction rates (Jennewein et al., 2005; Ponnamperuma & Croteau, 1996; Rana et al., 2013; Ro et al., 2002; Rosco, Pauli, Priesner, & Kutchan, 1997; Waheed Bhat et al., 2014; Zhou, Zhou, & Li, 2021). For instance, when rat and mung bean CPRs were used to couple with mint (*Mentha piperita*) CYP genes, which encode limonene hydroxylases, limonene could not be reliably converted to trans-carveol or trans-isopiperitenol (Ponnamperuma & Croteau, 1996). By contrast, CPR from spearmint (*M. spicata*), a close relative of *M. piperita*, was capable of catalysing the hydroxylation of limonene in association with *M. piperita* CYPs (Ponnamperuma & Croteau, 1996).

Plant CPRs are also highly favoured for production of plant natural products within *E. coli* and yeast for synthetic biology (M.C.Y. Chang, Eachus, Trieu, Ro, & Keasling, 2007; Ro et al., 2008; Waheed Bhat et al., 2014; Walters Biggs et al., 2016). For example, when *A. annua* CPR1 was used to replace a yeast CPR to pair with its native redox partner, amorpha-4,11-diene oxygenase (CYP71AV1) in *S. cerevisiae*, the production of artemisinin precursors was increased 12-fold (M.C.Y. Chang et al., 2007).

CPR paralogues from the same plant species have also exhibited preferential CYP catalysis (Park, Kim, Rupasinghe, Schuler, & Back, 2013; Su et al., 2017). For example, three CPR genes from rice (*Oryza sativa*), namely *OsCPR1*, *OsCPR2*, and *OsCPR3*, which categorise into the CPR2 clade (refer Fig. 4), were cloned and expressed in *E. coli* (Park et al., 2013). When each of them was co-induced with a tryptamine 5-hydroxylase (T5H), encoded by *CYP71P1*, the pairing of OsCPR2 and T5H increased the production of serotonin 12-fold and 4-fold higher than OsCPR3 and T5H and OsCPR1 and T5H (Park et al., 2013). Their divergent activity was also observed in the co-expression of *CYP73A1* encoding cinnamate 4-hydroxylase (C4H), which catalyses an entry step of the phenylpropanoid pathway. OsCPR2 and C4H were more effective at hydroxylating cinnamic acid to *p*-coumaric acid than both OsCPR1 and C4H and OsCPR3 and C4H (Park et al., 2013). Likewise, similar results were observed for four CPR paralogues from *Tripterygium wilfordii* (TwCPR1–TwCPR4), all of which supported *ent*-kaurenoic acid production, a gibberellin intermediate, when paired with CYP701A (Su et al., 2017). Of the four pairs, TwCPR3 and CYP701A produced the most *ent*-kaurenoic acid followed by TwCPR4 and CYP701A (Su et al., 2017). The contributions of TwCPR1 and TwCPR2 with CYP701A to gibberellin biosynthesis were lower than CPR3 and 4 (Su et al., 2017). Since TwCPR3 groups into the CPR1

clade (refer Fig. 4), its elevated involvement in *T. wilfordii* primary metabolism (gibberellin biosynthesis) is consistent with previous reports on CPR1 activity (Parage et al., 2016; Ro et al., 2002; Urban et al., 1997). Nevertheless, its capacity to outcompete TwCPR4, another CPR1 paralogue, in the CYP701A interaction demonstrates that CYP preferences also exist among CPR1 paralogues.

While CPRs are demonstrably important for efficient CYP catalysis, one report also showed that CPR identity affected the stereochemical outcome of CYP reaction products (Kraus & Kutchan, 1995). Within an insect cell model (*Spodoptera frugiperda*), berbamunine synthase (*CYP80A1*) from *Berberis stolonifera*, was paired with the native insect *CPR* (*SfCPR*) and *B. stolonifera CPR* (*BsCPR*) (Kraus & Kutchan, 1995). Depending on the CPR used, CYP80A1 catalysed the oxidative dimerisation of enantiomer reactants (R)-N-methylcoclaurine and (S)-N-methylcoclaurine into varying ratios of (R, R) and (R, S) stereodimers (Kraus & Kutchan, 1995). Under equimolar amounts of reactants, in the presence of SfCPR, the ratio of (R, R) to (R, S) was 85:15. In the presence of BsCPR, the ratio of (R, R) to (R, S) was 62:38 (Kraus & Kutchan, 1995). These data indicate that although CPRs use a similar mechanism for ET and reduction of CYPs, different CPR origins exhibit divergent roles not only in catalytic efficiency but also in the stereo configuration of catalytic products. This is especially pertinent in plants given their extensive stereochemical diversity, as reflected by, C-ring oriented strigolactones (diastereomers) (Homma et al., 2024), neolignans (enantiomers) (Hu, Diao, & Liang, 2026; Y. Lu et al., 2015), and key chiral intermediates for tropane alkaloid biosynthesis (e.g., tropinone, cocaine) (Bedewitz, Jones, D'Auria, & Barry, 2018), and terpenoids. Since numerous CYPs are involved in the synthesis of these molecules (Bedewitz et al., 2018; Homma et al., 2024; Hu et al., 2026; Kraus & Kutchan, 1995; Y. Lu et al., 2015), one hypothesis is that CPR paralogues from one plant, or homologues from different plant species, might play fundamental roles in stereo configurations of plant secondary metabolites.

4 Structural Variations Associated with Functional Divergence of Plant CPRs

While research is beginning to show functional divergence among CPR paralogues in plants, the mechanisms behind these differences are not well understood. To date only two plant CPRs, ATR2 from Arabidopsis (Niu et al., 2017) and SbCPR2b from sorghum (B. Zhang et al., 2022), have been crystallised. Consequently, most of the work on CPR conformations, docking simulations, and their variants has involved rat and human CPR, for which multiple crystal structures exist (Deeni et al., 2001; Djordjevic et al., 1995; Q. Zhao et al., 1996). Mammalian CPRs therefore serve as an appropriate benchmark for determining the biochemical, structural, and biophysical components that drive CPR functional diversity in plants.

The domains and residues responsible for the diverse properties of CPRs are quite varied according to the literature. CPR has been modified and altered across each of its major domains and binding regions: the anchor/transmembrane domain, the FMN-binding domain, the FAD-binding domain, the NADPH-binding domain, and the connecting domain/inter-domain regions (Aigrain, Pompon, & Truan, 2011;

S.B. Jensen et al., 2021; Laursen et al., 2011; Miyamoto et al., 2015; Strohmaier et al., 2019; Ullrich, 1979).

4.1 The N-terminal Anchor

The N-terminal anchor of CPR is a hydrophobic transmembrane domain whose role is to localise and tether the enzyme to the cytosolic side of the ER membrane (Barnaba, Martinez, et al., 2017; Barnaba, Taylor, & Brozik, 2017). Its anchoring capacity and localisation are fundamental to ET and the spatial organisation and catalytic function of CYPs (Laursen et al., 2021). Due to its hydrophobicity, it is commonly removed for induction in *E. coli* as a truncated protein to increase its solubility (Cheng et al., 2023; Ebrecht et al., 2019; Lamb et al., 2006; Miyamoto et al., 2015; Murataliev et al., 2004; Park et al., 2013; Walters Biggs et al., 2016; B. Zhang et al., 2022; Zhou et al., 2021). When CPRs are truncated to remove the N-terminal anchoring domain for expression and purification from *E. coli*, two phenomena are observed. The first is that CPR interactions with cytochrome *c* are maintained and, in some cases, improved (Hamdane et al., 2009), and the second is that interactions with some CYPs and their substrates are either hindered or abolished (Campelo et al., 2017; Miyamoto et al., 2015; Ullrich, 1979; B. Zhang et al., 2022). It is thought that the release of CPR from the ER membrane after removal of the N-terminal anchor increases soluble cytochrome *c*'s access to its FMN domain since cytochrome *c* is no longer restricted by the ER membrane (Campelo et al., 2017). Consequently, this is considered a major determinant in the improved efficiency of ET between the two proteins (Miyamoto et al., 2015). These *in-vitro* data indicate that the anchor domain is important for subcellular metabolic activities.

Though the effects of the membrane anchor on CYP associations is less clear, one hypothesis is that the anchoring domain may help to orient and bind CPR to CYP for effective ET at the ER (Esteves et al., 2020; K. Jensen & Møller, 2010; Mukherjee, Nandekar, & Wade, 2021). One report, for instance, stated that human CPR in its truncated form changed its preferential binding to CYP2C19—a xenobiotic-metabolising CYP—depending on what drugs were present (Miyamoto et al., 2015). The binding of CYP2C19 to truncated CPR was increased when amitriptyline and imipramine (tricyclic antidepressants) were present but decreased in the presence of omeprazole and lansoprazole (proton pump inhibitors) (Miyamoto et al., 2015). Notably, the metabolic activity of truncated CPR was effectively lost in the presence of omeprazole and lansoprazole (Miyamoto et al., 2015). This loss of activity was attributed to the diversion of electrons to oxidative shunt pathways (i.e., which produce O_2^-, H_2O_2, and H_2O) (Miyamoto et al., 2015). The basal level of H_2O_2 production for truncated and non-truncated CPR with CYP2C19 in the absence of drugs was approximately 40µM. When amitriptyline and imipramine were included in the reaction with truncated CPR, H_2O_2 levels dropped to 20µM, and with the addition of omeprazole and lansoprazole, H_2O_2 levels increased to 40µM and 45µM, respectively (Miyamoto et al., 2015). Conversely, non-truncated CPR effectively maintained lower H_2O_2 levels at all drug conditions (Miyamoto et al., 2015). Thus, it was proposed that the membrane anchor assumes a more integral biochemical role by suppressing the loss of electrons to oxidative shunt pathways (Miyamoto et al., 2015).

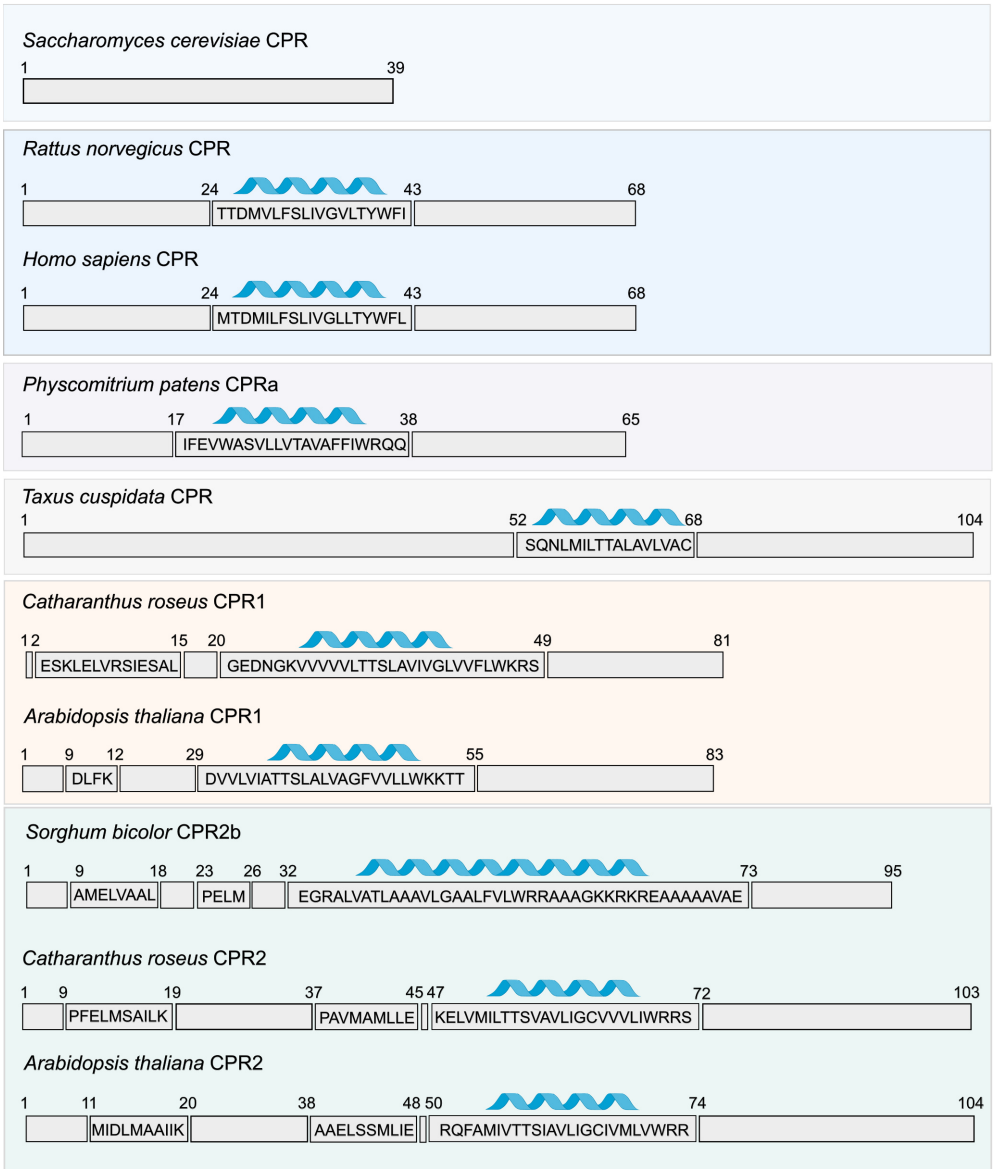

Fig. 5 Comparison of CPR hinge variations between (A) *A. thaliana* ATR1 (orange) and ATR2 (teal) and (B) *Artemisia annua* AaCPR1 (grey) and AaCPR2 (teal). The hinges are more opaque than the rest of the enzyme, are lightly outlined in black, and form loops. Tables on the right depict the residue order from the FMN domain facing side of the hinge to the connecting domain facing side. Residue differences are highlighted in teal. ATR1 (primary metabolism) and ATR2 (secondary metabolism) are phylogenetically divergent and have greater variability at the hinge with eight residue differences. Conversely, AaCPR1 and AaCPR2 only have two residue differences.

Despite the lack of conservation among residues at the N-terminal anchor, it is evident that residue identity within this region does modulate CYP and substrate interactions. This feature has been indirectly validated by truncation experiments. One previous study has shown that different truncations of CPR paralogues caused them to vary in their substrate turnover abilities (Park et al., 2013). For instance, rice OsCPR2 exhibited a 22% and 50% reduction in serotonin production with CYP71P when the first 25 and 105 amino acids were deleted, while OsCPR1 exhibited a 50% reduction in serotonin production when only 79 amino acids were deleted (Park et al., 2013). The different activities resulting from the two truncations were likely due to changes to the electrostatic potential and hydrophobic properties of CPR after removal of certain residues (Campelo et al., 2018; K. Jensen & Møller, 2010; Park et al., 2013; X. Zhao et al., 2023). Furthermore, the two types of truncation may have contributed to alterations of the anchor's flexibility (Lepesheva, Hargrove, & Ren, 2026; Wang et al., 1997). Although the potential roles of anchor flexibility remain uncharacterised, the flexibility of other unstructured regions (e.g., hinge) within CPR proteins have been implicated in CYP preferential partnerships (Campelo et al., 2018, 2017; Esteves et al., 2020).

One *in-vivo* study demonstrated that the N-terminal α-helical motif (residues 25–45) of human CPR limits its lateral diffusion within the ER membrane (Barnaba, Martinez, et al., 2017). This is likely because of the motif's hydrophobic amino acid composition. While plant CPRs also demonstrate membrane-spanning, hydrophobic α-helices (refer Fig. 5), their effects on CPR diffusion through the ER membrane have not yet been characterised. Plants have longer N-terminal anchors than mammalian CPRs (e.g., rat and human), which can sometimes reach lengths of 100 residues or more (refer Fig. 5) (Parage et al., 2016; Ro et al., 2002). Additionally, though mammalian CPRs possess compact ∼20-residue N-terminal transmembrane anchors, plant CPRs are predicted to contain slightly extended hydrophobic regions and additional flanking residues, suggesting greater sequence and structural diversity in ER membrane anchoring (refer Fig. 5). Plant CPR1 and CPR2 anchors, for example, are also known to differ on the basis of CPR2's longer length and serine and threonine enriched residues (Parage et al., 2016; Ro et al., 2002; B. Zhang et al., 2022). This type of residue variation might also contribute to the differentiating roles of CPR1 and CPR2 in plant primary and secondary metabolism. Altogether, differences in hydrophobicity, electrostatic potential, and flexibility provide a useful starting point for uncovering the unique qualities of plant CPR N-termini.

4.2 Features of the FMN Binding Domain, Hinge, and Connecting Domain and Their Roles in CPR Flexibility and Enzyme Partnering

The NADPH binding site is contained within the same structural unit as the FAD binding domain (e.g., FNR module or FAD/NADPH binding domain) (Grunau, Geraki, Grossmann, & Gutierrez, 2007). Thus, alterations within this region can impact FAD and NADPH co-factor binding and subsequent CPR activity (Strohmaier et al., 2019; C. Xia et al., 2011, 2018). Such alterations can cause either negative or positive effects on CPR activity.

In human *CPR*, two naturally occurring missense mutations cause amino acid substitutions, V492E and R457H (C. Xia et al., 2011). Though structurally similar to the wild-type, these variants demonstrate disruptions in H bonding and salt bridging that weaken the capacity for FAD binding and lead to enzyme destabilisation and loss of catalysis (C. Xia et al., 2011). Moreover, the differential unfolding properties of the two variants are reflected in their variable stability. The variant V492E, though less stable, has been shown to unfold locally, whereas the more stable R457H variant has been shown to unfold globally (C. Xia et al., 2011). These two variants reveal how single amino acid variations can affect the binding and stabilising properties of CPRs. Fortunately, the negative effects associated with these variations can be compensated for by the addition of more FAD (C. Xia et al., 2011). This reinforces the essentialness of co-factor binding for ensuring CPR stability.

Not all FAD/NADPH binding domain variations have negative effects. In comparison with natural human CPR variants, three derived CPR variants, R597M, K602D, and W676A, showed four-fold increases in catalytic efficiency toward CYP2A6 and CYP2C9 (Strohmaier et al., 2019). Contrary to the earlier understanding that improvements in CYP catalysis must be based close to the predicted interaction site (e.g., the FMN domain), this study contributed to the understanding that CPR-CYP catalysis can be influenced by variations across other domains.

The binding and release of NADPH has now been attributed to CPR conformational changes based on its redox state (Strohmaier et al., 2019; C. Xia et al., 2018; S. Xia & Hirao, 2024; B. Zhang et al., 2022). In particular, the human CPR Asp632 loop (G631-N635) in the NADPH binding region has been implicated in domain movement (C. Xia et al., 2018). Apart from NR1, this residue is conserved among other investigated diflavin reductase members (C. Xia et al., 2018). A residue substitution of D632A/F in hCPR altered the conformational movements of the Asp loop, positioning of the NADPH nicotinamide ring, H-bonding with the conserved W677 residue (refer Fig. 2-3), and the distance between the FAD and FMN co-factors (C. Xia et al., 2018). These data reveal that D632 plays an essential role in NADPH mediated CPR movements and efficient catalysis with CYP.

While similar studies are limited among plant CPRs, the positioning of $NADP^+$ in SbCPR2b (sorghum CPR2b) crystals was found to be much more defined than what has been observed in oxidised human and rat CPR crystals, which have shown only disordered $NADP^+$ (C. Xia et al., 2018; B. Zhang et al., 2022). Only when reduced, did hCPR reveal a clear placement of $NADP^+$ (C. Xia et al., 2018). This suggests that NADPH binding modes differ among mammalian and plant CPRs, which may confer downstream differences in FMN domain motions. Furthermore, based on $NADP^+$ bound and free structures, Zhang et al. (2022) proposed that the Asp-loop conformational change does not occur in plants. Therefore, it is possible that plants possess another mechanism for NADP binding and release. Whether such a mechanism varies among plant CPR paralogues requires further study.

4.3 The Structure of the Hinge Facilitates CPR Flexibility and Enzyme Partnering

The FMN binding domain and its position are a key determinant of CPR function (Esteves et al., 2023; Hamdane et al., 2009; Hubbard, Shen, Paschke, Kasper, & Kim, 2001; Strohmaier et al., 2019; Udhane, Parween, Kagawa, & Pandey, 2017; B. Zhang et al., 2022). Various crystal structures have been solved which illustrate the highly mobile nature of this domain. The assembly of those structures reveals a spectrum of CPR conformational states from open to closed (Hamdane et al., 2009; Haque et al., 2014; Wang et al., 1997). These assemblies are dictated by the CPR redox state as it shuttles electrons from FMN to FAD (closed conformation) and then to a terminal electron acceptor (open conformation) (Haque et al., 2014; Huang, Ellis, Moody, Raven, & Roberts, 2013; Lepesheva et al., 2026).

A recent investigation of oxidised rat CPR with cryogenic electron microscopy (cryo-EM) revealed that its crystals, when in their oxidised state, formed a minimum of five distinct closed conformations, in which the N5-to-N5 distances between the FAD and FMN co-factors, were 15 Å (∼42% of particles), 16 Å (∼29%), 17 Å (∼15%), 18 Å (∼9%), and 22 Å (∼5%) (Lepesheva et al., 2026). Likewise, analysis of fully reduced SbCPR2b (sorghum) with small molecule Fluorescence Resonance Energy Transfer (smFRET) and homology modelling revealed that it formed five different conformational states (S1-S5) at equilibrium: S1 (occupying 17% of the conformations present), S2 (25%), S3 (16%), S4 (27%) and S5 (14%) (S.B. Jensen et al., 2021). Although the mechanisms behind the formation of these many conformations remain open for characterisation, it has been proposed that this phenomenon is both homologue- (Lepesheva et al., 2026; Niu et al., 2017; B. Zhang et al., 2022), redox state- (Haque et al., 2014; Huang et al., 2013), and substrate-dependent (S.B. Jensen et al., 2021).

A

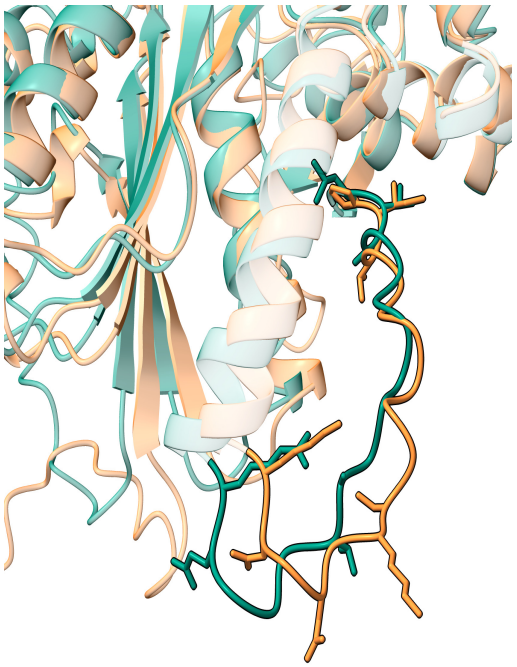

ATR1	ATR2
Lys243	Arg263
Asp244	Glu264
Glu245	Glu265
Asp246	Gly266
Asp247	Asp267
Lys248	Thr268
Ser249	Ala269
Val250	Val270
Ala251	Ala271
Thr252	Thr272
Pro253	Pro273
Tyr254	Tyr274
Thr255	Thr275
Ala256	Ala276
Val257	Ala277
Ile258	Val278
Pro259	Leu279
Glu260	Glu280
Tyr261	Tyr281

B

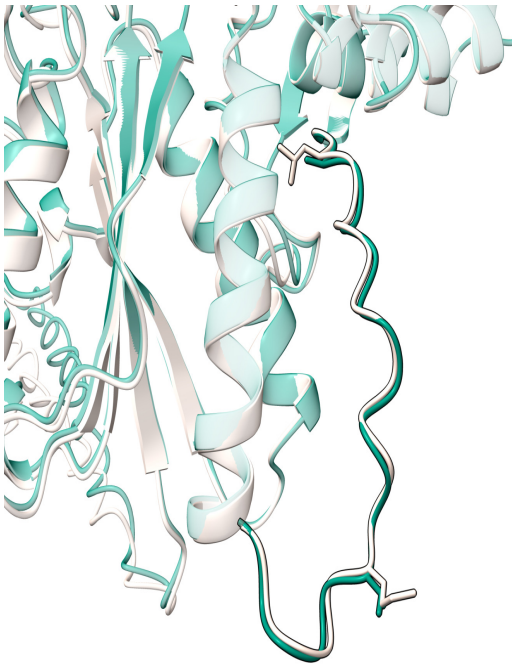

AaCPR1	AaCPR2
Leu257	Leu261
Arg258	Arg262
Asp259	Asp263
Glu260	Glu264
Asp261	Asp265
Asp262	Asp266
Thr263	Met267
Ser264	Ser268
Val265	Val269
Ala266	Ala270
Thr267	Thr271
Pro268	Pro272
Tyr269	Tyr273
Thr270	Thr274
Ala271	Ala275
Ala272	Ala276
Val273	Val277
Ala274	Leu278
Glu275	Glu279
Tyr276	Tyr280

Fig. 6 Comparison of CPR hinge variations between (A) *A. thaliana* ATR1 (orange) and ATR2 (teal) and (B) *Artemisia annua* AaCPR1 (grey) and AaCPR2 (teal). The hinges are more opaque than the rest of the enzyme, are lightly outlined in black, and form loops. Tables on the right depict the residue order from the FMN domain facing side of the hinge to the connecting domain facing side. Residue differences are highlighted in teal. ATR1 (primary metabolism) and ATR2 (secondary metabolism) are phylogenetically divergent and have greater variability at the hinge with eight residue differences. Conversely, AaCPR1 and AaCPR2 only have two residue differences.

A major component of CPRs that facilitates opening and closing between the NADPH/FAD and FMN domains is the flexible hinge. The amino acid composition of the CPR hinge is vital for the formation of dynamic shapes for CPR to perform redox reactions (Campelo et al., 2018, 2017). Although all CPRs have hinge regions, differences exist across different homologues. Additionally, one report predicted that plant CPRs contain more flexible hinges than mammalian CPRs (B. Zhang et al., 2022). Despite the lack of data to support this hypothesis, past structural analysis of proteins provides valuable preliminary evidence. For instance, among the two solved plant crystal structures—ATR2 (Arabidopsis) (Niu et al., 2017) and SbCPR2b (sorghum) (B. Zhang et al., 2022)—neither were able to resolve a long disordered region that encompassed the CPR hinge and part of the connecting domain. In mammalian CPRs this region has approximately 10 residues, whereas in ATR2 (AtCPR2) it is 43 residues (B. Zhang et al., 2022).

X-ray crystallography and cryo-EM often fail to resolve these segments because of their high conformational flexibility, resulting in weak or absent electron density in crystallographic maps or poorly resolved density in cryo-EM reconstructions (Lepesheva et al., 2026). The hinge and connecting domain therefore contribute to differences in flexibility between mammalian and plant CPRs. The catalytic importance of the CPR hinge was first proposed by (Hamdane et al., 2009) and has since been recapitulated by other groups (Aigrain et al., 2011; Campelo et al., 2017; Esteves et al., 2020; S.B. Jensen et al., 2021; B. Zhang et al., 2022). A four amino acid deletion in the rCPR hinge resulted in a permanent open conformation. This has led to the understanding that the hinge acts as a flexible point of contact between the FMN, FAD, and NADPH binding domains (Laursen et al., 2011). This flexibility/conformational modulation has been reported to influence CPR interactions with CYP partners (Campelo et al., 2018, 2017; Laursen et al., 2011). When Campelo et al. (2017) tested several human CPR (hCPR) FMN-FAD hinge variants with common CYPs, they found that rather than abolishing CYP interactions, the CPRs demonstrated selectivity for one CYP over another. For example, the I245F variant increased catalysis of two CYPs but decreased catalysis of two others (Campelo et al., 2018).

A comparison of this region between ATR1 (CPR1) and ATR2 (CPR2) of Arabidopsis revealed an 8 amino acid difference at the hinge (refer Fig. 6). Conversely, the two CPR2 paralogues of *A. annua* differed by two amino acids at the hinge (refer Fig. 6). These hinge differences reflect not only the degree of relatedness for CPR paralogues but may also support the diversification of these enzymes into different aspects of plant metabolism. ATR1 (AtCPR1) and ATR2 (AtCPR2) diverge into primary and secondary metabolism, respectively, and thus, their hinge differences are greater than AaCPR1 and AaCPR2. However, as demonstrated in the hCPR hinge variants, the two residue substitutions between AaCPR1 and AaCPR2 could still sufficiently alter hinge flexibility enough that they exhibit different CYP preferences.

5 Conclusion

Recapitulating the functional divergence of plant CPRs is challenging. Their domains do not function in isolation. As Strohmaier et al. (2019) discovered, residue changes far

from the catalytic site can still have effects on CPR-CYP dynamics. Current research supports the idea that any changes to CPR enzymes which alter their conformational capacity will have an effect on ET, CYP preference, and catalytic potential (Campelo et al., 2017; Haque et al., 2014; Huang et al., 2013; S.B. Jensen et al., 2021; Strohmaier et al., 2019; X. Zhao et al., 2023). Altogether, these studies reveal that CPR-CYP dynamics are far more complicated than previously proposed and that the different domains of CPR must work together and modulate co-factor and CYP binding in a substrate-, and CYP-dependent manner. The finding that CPR co-exists in equilibrium with conformational variants of itself *in-vitro* (Haque et al., 2014; Huang et al., 2013; S.B. Jensen et al., 2021; Lepesheva et al., 2026), sheds light on a potential mechanism for CPR-CYP selectivity and catalysis. A substitution of two amino acids in hCPR increased the proportion of its open conformation (*in-vitro*) (Huang et al., 2013) and substrate binding is known to shift conformational states in SbCPR2b (*in-vivo*) (S.B. Jensen et al., 2021). This suggests that CPR functional divergence may be dependent on the abundance of its respective conformational states, which change based on electrostatic and redox potential and substrate/co-factor binding. The CYP and substrate dependent activities of CPR were described by Jensen et al. (2021) as biased metabolism. While the smFRET data on SbCPR2b and its conformational states attempted to mimic a lipid environment by integrating the enzyme into nanodiscs, there are no known studies that show multiple CPR conformational states *in-vivo*. Studies of this nature will be necessary to fully reconcile CPR behaviour and divergence among plant CPR paralogues within a biological context. Moreover, research into CPR domain functions and mechanisms have come mainly from human or rat CPRs—with the exception of sorghum CPR. This presents a knowledge gap concerning the untapped potential in plant CPRs to account for CYP dependencies and the ways that this can differentially modulate plant metabolism.

Despite belonging to a small protein family, CPRs are essential to ET for CYP-mediated metabolic processes in all organisms. Given their indispensable roles in CYP catalysis, as described above, human CPR and other known CPRs have been extensively studied in molecular biology, genomics, genetics, and biochemistry. In comparison, the biophysical properties of CPRs and their roles in the formation of transient conformational shapes, largely remain open for characterisation. In particular, although active domains have been functionally determined, the role of hinges and connecting domain loops in different homologues and among paralogues in the same species needs to be further elucidated in the future. Additionally, the stoichiometry of CPR and CYPs in the same cells and different cells of an organism need to be determined. The resulting data will be fundamental not only for understanding the redox efficiency of CPR and CYPs but also for innovating CPR and CYP variants for metabolic engineering.

References

Aigrain, L., Fatemi, F., Frances, O., Lescop, E., Truan, G. (2012). Dynamic control of electron transfers in diflavin reductases. *International Journal of Molecular Sciences*, *13*, ,

Aigrain, L., Pompon, D., Moréra, S., Truan, G. (2009). Structure of the open conformation of a functional chimeric nadph cytochrome p450 reductase. *EMBO Reports*, *10*, 742–747, https://doi.org/10.1038/embor.2009.82

Aigrain, L., Pompon, D., Truan, G. (2011). Role of the interface between the fmn and fad domains in the control of redox potential and electronic transfer of nadph-cytochrome p450 reductase. *Biochemical Journal*, *435*, 197–206, https://doi.org/10.1042/BJ20101984

Barnaba, C., Martinez, M.J., Taylor, E., Barden, A.O., Brozik, J.A. (2017). Single-protein tracking reveals that nadph mediates the insertion of cytochrome p450 reductase into a biomimetic of the endoplasmic reticulum. *Journal of the American Chemical Society*, , https://doi.org/10.1021/jacs.7b00663

Barnaba, C., Taylor, E., Brozik, J.A. (2017). Dissociation constants of cytochrome p450 2c9/cytochrome p450 reductase complexes in a lipid bilayer membrane depend on nadph: A single-protein tracking study. *Journal of the American Chemical Society*, *139*, 17923–17934, https://doi.org/10.1021/jacs.7b08750

Bassila, C., Ghemrawi, R., Flayac, J., Froese, D.S., Baumgartner, M.R., Guéant, J.L., Coelho, D. (2017). Methionine synthase and methionine synthase reductase interact with mmachc and with mmadhc. *Biochimica et Biophysica Acta - Molecular Basis of Disease*, *1863*, 103–112, https://doi.org/10.1016/j.bbadis.2016.10.016

Bedewitz, M.A., Jones, A.D., D'Auria, J.C., Barry, C.S. (2018). Tropinone synthesis via an atypical polyketide synthase and p450-mediated cyclization. *Nature Communications*, *9*, , https://doi.org/10.1038/s41467-018-07671-3

Benveniste, I., Lesot, A., Hasenfratz, M.-P., Kochs, G., Durst, F. (1991). Multiple forms of nadph cytochrome p450 reductase in higher plants. *Biochemical and Biophysical Research Communications*, *177*, 105–112,

Brown, S., Clastre, M., Courdavault, V., O'Connor, S.E. (2015). De novo production of the plant-derived alkaloid strictosidine in yeast. *Proceedings of the National Academy of Sciences of the United States of America*, *112*, 3205–3210, https://doi.org/10.1073/pnas.1423555112

Campelo, D., Esteves, F., Palma, B.B., Gomes, B.C., Rueff, J., Lautier, T., et al. (2018). Probing the role of the hinge segment of cytochrome p450 oxidoreductase in the interaction with cytochrome p450. *International Journal of Molecular Sciences*, *19*, , https://doi.org/10.3390/ijms19123914

Campelo, D., Lautier, T., Urban, P., Esteves, F., Bozonnet, S., Truan, G., Kranendonk, M. (2017). The hinge segment of human nadph-cytochrome p450 reductase in conformational switching: The critical role of ionic strength. *Frontiers in Pharmacology*, *8*, , https://doi.org/10.3389/fphar.2017.00755

Chang, M.C.Y., Eachus, R.A., Trieu, W., Ro, D.-K., Keasling, J.D. (2007). Engineering Escherichia coli for production of functionalized terpenoids using plant p450s. *Nature Chemical Biology*, *3*, 274–277, https://doi.org/10.1038/nchembio875

Chang, Z., Wang, X., Wei, R., Liu, Z., Shan, H., Fan, G., Hu, H. (2018). Functional expression and purification of cyp93c20, a plant membrane-associated cytochrome p450 from Medicago truncatula. *Protein Expression and Purification*, , https://doi.org/10.1016/j.pep.2018.04.017

Chen, R., Gao, J., Yu, W., Chen, X., Zhai, X., Chen, Y., et al. (2022). Engineering cofactor supply and recycling to drive phenolic acid biosynthesis in yeast. *Nature Chemical Biology*, *18*, 520–529, https://doi.org/10.1038/s41589-022-01014-6

Chen, X., Luo, X., Cao, F., Zhu, T., Fan, Y., Jia, X., Shen, Y. (2014). Molecular cloning, expression of cpr gene from Rhizopus oryzae into Rhizopus nigricans and its application in the 11alpha-hydroxylation of 16alpha,17-epoxyprogesterone. *Enzyme and Microbial Technology*, *66*, 28–34, https://doi.org/10.1016/j.enzmictec.2014.08.002

Cheng, J., Li, G., Wang, X., Yang, C., Xu, F., Qian, Z., Ma, X. (2023). Cloning and functional characterization of nadph-cytochrome p450 reductases in Aconitum vilmorinianum. *Molecules*, *28*, , https://doi.org/10.3390/molecules28217409

Choi, W., Park, S.Y., Kim, H.M., Mai, T.D., Do, J.H., Jang, H.M., et al. (2023). Heterologous expression in Escherichia coli and functional characterization of the tomato cpr enzymes. *Applied Biological Chemistry*, *66*, 92, https://doi.org/10.1186/s13765-023-00850-x

Deeni, Y.Y., Paine, M.J., Ayrton, A.D., Clarke, S.E., Chenery, R., Wolf, C.R. (2001). Expression, purification, and biochemical characterization of a human cytochrome p450 cyp2d6-nadph cytochrome p450 reductase fusion protein. *Archives of Biochemistry and Biophysics*, *396*, 16–24, https://doi.org/10.1006/abbi.2001.2585

Deng, Z., Aliverti, A., Zanetti, G., Arakaki, A.K., Ottado, J., Orellano, E.G., et al. (1999). A productive nadp$^+$ binding mode of ferredoxin-nadp$^+$ reductase revealed by protein engineering and crystallographic studies. *Nature Structural Biology*, *6*, 847–853, https://doi.org/10.1038/12307

Djordjevic, S., Roberts, D.L., Wang, M., Shea, T., Cammer, M.G.W., Masters, B.S.S., Estabrook, R.W. (1995). Crystallization and preliminary x-ray studies of nadph-cytochrome p450 reductase (x-ray crystallography/flavoprotein). *Proceedings of the National Academy of Sciences of the United States of America*, *92*, 3214–3218,

Ebrecht, A.C., van der Bergh, N., Harrison, S.T., Smit, M.S., Sewell, B.T., Opperman, D.J. (2019). Biochemical and structural insights into the cytochrome p450 reductase from Candida tropicalis. *Scientific Reports*, *9*, , https://doi.org/10.1038/s41598-019-56516-6

Ershov, P.V., Yablokov, O., Florinskaya, A.V., Mezentsev, Y.V., Kaluzhskiy, L., Tumilovich, A.M., et al. (2019). Spr-based study of affinity of cytochrome p450s/redox partner interactions modulated by steroidal substrates. *Journal of Steroid Biochemistry and Molecular Biology*, *187*, 124–129, https://doi.org/10.1016/j.jsbmb.2018.11.009

Esteves, F., Almeida, C.M., Silva, S., Saldanha, I., Urban, P., Rueff, J., et al. (2023). Single mutations in cytochrome p450 oxidoreductase can alter the specificity of human cytochrome p450 1a2-mediated caffeine metabolism. *Biomolecules*, *13*, 1083, https://doi.org/10.3390/biom13071083

Esteves, F., Campelo, D., Gomes, B.C., Urban, P., Bozonnet, S., Lautier, T., et al. (2020). The role of the fmn-domain of human cytochrome p450 oxidoreductase in its promiscuous interactions with structurally diverse redox partners. *Frontiers in Pharmacology*, *11*, , https://doi.org/10.3389/fphar.2020.00299

Grinkova, Y.V., Denisov, I.G., McLean, M.A., Sligar, S.G. (2012). Oxidase uncoupling in heme monooxygenases: Human cytochrome p450 cyp3a4 in nanodiscs. *Biochemical and Biophysical Research Communications*, *430*, 1223–1228, https://doi.org/10.1016/j.bbrc.2012.12.072

Grunau, A., Geraki, K., Grossmann, J.G., Gutierrez, A. (2007). Conformational dynamics and the energetics of protein-ligand interactions: Role of interdomain loop in human cytochrome p450 reductase. *Biochemistry*, *46*, 8244–8255, https://doi.org/10.1021/bi700596s

Gu, M., Wang, M., Guo, J., Shi, C., Deng, J., Huang, L., et al. (2019). Crystal structure of cyp76ah1 in 4-π-bound state from Salvia miltiorrhiza. *Biochemical and Biophysical Research Communications*, *511*, 813–819, https://doi.org/10.1016/j.bbrc.2019.02.103

Guengerich, F.P. (2002). Rate-limiting steps in cytochrome p450 catalysis. *Biological Chemistry*, *383*, 1553–1564, https://doi.org/10.1515/BC.2002.175

Hamberger, B., & Bak, S. (2013). Plant p450s as versatile drivers for evolution of species-specific chemical diversity. *Philosophical Transactions of the Royal Society B: Biological Sciences*, *368*, 1–16, https://doi.org/10.1098/rstb.2012.0426

Hamdane, D., Xia, C., Im, S.C., Zhang, H., Kim, J.J.P., Waskell, L. (2009). Structure and function of an nadph-cytochrome p450 oxidoreductase in an open conformation capable of reducing cytochrome p450. *Journal of Biological Chemistry*, *284*, 11374–11384, https://doi.org/10.1074/jbc.M807868200

Hansen, C.C., Sørensen, M., Veiga, T.A., Zibrandtsen, J.F., Heskes, A.M., Olsen, C.E., et al. (2018). Reconfigured cyanogenic glucoside biosynthesis in Eucalyptus cladocalyx involves a cytochrome p450 cyp706c55. *Plant Physiology*, *178*, 1081–1095, https://doi.org/10.1104/pp.18.00998

Haque, M.M., Bayachou, M., Tejero, J., Kenney, C.T., Pearl, N.M., Im, S.C., et al. (2014). Distinct conformational behaviors of four mammalian dual-flavin reductases (cytochrome p450 reductase, methionine synthase reductase, neuronal nitric oxide synthase, endothelial nitric oxide synthase) determine their unique catalytic profiles. *FEBS Journal*, *281*, 5325–5340, https://doi.org/10.1111/febs.13073

Homma, M., Wakabayashi, T., Moriwaki, Y., Shiotani, N., Shigeta, T., Isobe, K., et al. (2024). Insights into stereoselective ring formation in canonical strigolactone: Identification of a dirigent domain-containing enzyme catalyzing orobanchol synthesis. *Proceedings of the National Academy of Sciences of the United States of America*, *121*, e2313683121, https://doi.org/10.1073/pnas.2313683121

Hu, Y.J., Diao, N., Liang, D. (2026). Flavonoid derivatives and lignan enantiomers from Phanera championii benth. and their anti-neuroinflammatory activity. *Phytochemistry*, *247*, 114836, https://doi.org/10.1016/j.phytochem.2026.114836

Huang, W.C., Ellis, J., Moody, P.C., Raven, E.L., Roberts, G.C. (2013). Redox linked domain movements in the catalytic cycle of cytochrome p450 reductase. *Structure*, *21*, 1581–1589, https://doi.org/10.1016/j.str.2013.06.022

Hubbard, P.A., Shen, A.L., Paschke, R., Kasper, C.B., Kim, J.J.P. (2001). Nadph-cytochrome p450 oxidoreductase: Structural basis for hydride and electron transfer. *Journal of Biological Chemistry*, *276*, 29163–29170, https://doi.org/10.1074/jbc.M101731200

Iyanagi, T., Xia, C., Kim, J.J.P. (2012). Nadph-cytochrome p450 oxidoreductase: Prototypic member of the diflavin reductase family. *Archives of Biochemistry and Biophysics*, *528*, 72–89, https://doi.org/10.1016/j.abb.2012.09.002

Jennewein, S., Park, H., DeJong, J.H.M., Long, R.M., Bollon, A.P., Croteau, R.B. (2005). Coexpression in yeast of taxus cytochrome p450 reductase with cytochrome p450 oxygenases involved in taxol biosynthesis. *Biotechnology and Bioengineering*, *89*, 588–598, https://doi.org/10.1002/bit.20390

Jensen, K., & Møller, B.L. (2010). Plant nadph-cytochrome p450 oxidoreductases. *Phytochemistry*, *71*, 132–141, https://doi.org/10.1016/j.phytochem.2009.10.017

Jensen, S.B., Thodberg, S., Parween, S., Moses, M.E., Hansen, C.C., Thomsen, J., et al. (2021). Biased cytochrome p450-mediated metabolism via small-molecule ligands binding p450 oxidoreductase. *Nature Communications*, *12*, , https://doi.org/10.1038/s41467-021-22562-w

Karunanithi, P.S., Dhanota, P., Addison, J.B., Tong, S., Fiehn, O., Zerbe, P. (2019). Functional characterization of the cytochrome p450 monooxygenase cyp71au87 indicates a role in marrubiin biosynthesis in the medicinal plant Marrubium vulgare. *BMC Plant Biology*, *19*, , https://doi.org/10.1186/s12870-019-1702-5

Khanom, S., Jang, J., Lee, O.R. (2019). Overexpression of ginseng cytochrome p450 cyp736a12 alters plant growth and confers phenylurea herbicide tolerance in Arabidopsis. *Journal of Ginseng Research*, *43*, 645–653, https://doi.org/10.1016/j.jgr.2019.04.005

Kim, J.Y., Nakayama, M., Toyota, H., Kurisu, G., Hase, T. (2016). Structural and mutational studies of an electron transfer complex of maize sulfite reductase and ferredoxin. *The Journal of Biochemistry*, *160*, 101–109, https://doi.org/10.1093/jb/mvw016

Knosp, S., Kriegshauser, L., Tatsumi, K., Malherbe, L., Erhardt, M., Wiedemann, G., et al. (2024). An ancient role for cyp73 monooxygenases in phenylpropanoid biosynthesis and embryophyte development. *The EMBO Journal*, *43*, 4092, https://doi.org/10.1038/s44318-024-00181-7

Kraus, P.F.X., & Kutchan, T.M. (1995). *Molecular cloning and heterologous expression of a cdna encoding berbamunine synthase, a c-o phenol-coupling cytochrome p450 from the higher plant Berberis* (Tech. Rep.).

Krishnamurthy, P., Vishal, B., Bhal, A., Kumar, P.P. (2021). Wrky9 transcription factor regulates cytochrome p450 genes cyp94b3 and cyp86b1, leading to increased root suberin and salt tolerance in Arabidopsis. *Physiologia Plantarum*, *172*, 1673–1687, https://doi.org/10.1111/ppl.13371

Lah, L., Podobnik, B., Novak, M., Korošec, B., Berne, S., Vogelsang, M., et al. (2011). The versatility of the fungal cytochrome p450 monooxygenase system is instrumental in xenobiotic detoxification. *Molecular Microbiology*, *81*, 1374–1389, https://doi.org/10.1111/j.1365-2958.2011.07772.x

Lamb, D.C., Kim, Y., Yermalitskaya, L.V., Yermalitsky, V.N., Lepesheva, G.I., Kelly, S.L., et al. (2006). A second fmn binding site in yeast nadph cytochrome p450 reductase suggests a mechanism of electron transfer by diflavin reductases. *Structure*, *14*, 51–61, https://doi.org/10.1016/j.str.2005.09.015

Laursen, T., Borch, J., Knudsen, C., Bavishi, K., Torta, F., Martens, H.J., et al. (2016). Characterization of a dynamic metabolon producing the defense compound dhurrin in Sorghum. *Science*, *354*, 890–893, https://doi.org/10.1126/science.aag2347

Laursen, T., Jensen, K., Møller, B.L. (2011). Conformational changes of the nadph-dependent cytochrome p450 reductase in the course of electron transfer to cytochromes p450. *Biochimica et Biophysica Acta (BBA) - Proteins and Proteomics*, *1814*, 132–138, https://doi.org/10.1016/j.bbapap.2010.07.003

Laursen, T., Lam, H.Y.M., Sørensen, K.K., Tian, P., Hansen, C.C., Groves, J.T., et al. (2021). Membrane anchoring facilitates colocalization of enzymes in plant cytochrome p450 redox systems. *Communications Biology*, *4*, 1057, https://doi.org/10.1038/s42003-021-02604-1

Laursen, T., Møller, B.L., Bassard, J.E. (2015). Plasticity of specialized metabolism as mediated by dynamic metabolons. *Trends in Plant Science*, *20*, 20–32, https://doi.org/10.1016/j.tplants.2014.11.002

Lepesheva, G.I., Hargrove, T.Y., Ren, Y. (2026). Cryo-em reveals an ensemble of cytochrome p450 reductase conformations in solution. *Protein Science*, *35*, 1-11, https://doi.org/10.1002/pro.70448

Lesot, A., Benveniste, I., Hasenfratz, M.-P., Durst, F. (1990). Induction of nadph-cytochrome p-450 (c) reductase in wounded tissues from Helianthus tuberosus tubers. *Plant and Cell Physiology*, *31*, 1177–1182,

Lu, X., Shen, Q., Zhang, L., Zhang, F., Jiang, W., Lv, Z., et al. (2013). Promotion of artemisinin biosynthesis in transgenic Artemisia annua by overexpressing ads, cyp71av1 and cpr genes. *Industrial Crops and Products*, *49*, 380–385, https://doi.org/10.1016/j.indcrop.2013.04.045

Lu, Y., Xue, Y., Liu, J., Yao, G., Li, D., Sun, B., et al. (2015). (+-)-acortatarinowins a-f, norlignan, neolignan, and lignan enantiomers from Acorus tatarinowii. *Journal of Natural Products*, *78*, 2205–2214, https://doi.org/10.1021/acs.jnatprod.5b00328

Manoj, K.M., Gade, S.K., Mathew, L. (2010). Cytochrome p450 reductase: A harbinger of diffusible reduced oxygen species. *PLoS ONE*, *5*, e13272, https://

doi.org/10.1371/journal.pone.0013272

Mao, G., Seebeck, T., Schrenker, D., Yu, O. (2013). Cyp709b3, a cytochrome p450 monooxygenase gene involved in salt tolerance in Arabidopsis thaliana. *BMC Plant Biology*, *13*, 169, https://doi.org/10.1186/1471-2229-13-169

McClune, C.J., Liu, J.C.T., Wick, C., Peña, R.D.L., Lange, B.M., Fordyce, P.M., Sattely, E.S. (2025). Discovery of fot1 and taxol genes enables biosynthesis of baccatin iii. *Nature*, *643*, 582–592, https://doi.org/10.1038/s41586-025-09090-z

Meints, C.E., Simtchouk, S., Wolthers, K.R. (2013). Aromatic substitution of the fad-shielding tryptophan reveals its differential role in regulating electron flux in methionine synthase reductase and cytochrome p450 reductase. *FEBS Journal*, *280*, 1460–1474, https://doi.org/10.1111/febs.12141

Miller, J.C., Hollatz, A.J., Schuler, M.A. (2021). P450 variations bifurcate the early terpene indole alkaloid pathway in Catharanthus roseus and Camptotheca acuminata. *Phytochemistry*, *183*, 112626, https://doi.org/10.1016/j.phytochem.2020.112626

Miyamoto, M., Yamashita, T., Yasuhara, Y., Hayasaki, A., Hosokawa, Y., Tsujino, H., Uno, T. (2015). Membrane anchor of cytochrome p450 reductase suppresses the uncoupling of cytochrome p450. *Chemical and Pharmaceutical Bulletin*, *63*, 286–294, https://doi.org/10.1248/cpb.c15-00034

Monchietti, P., Rivero, A.S.L., Ceccarelli, E.A., Catalano-Dupuy, D.L. (2021). A new catalytic mechanism of bacterial ferredoxin-nadp+ reductases due to a particular nadp+ binding mode. *Protein Science*, *30*, 2106–2120, https://doi.org/10.1002/pro.4166

Mukherjee, G., Nandekar, P.P., Wade, R.C. (2021). An electron transfer competent structural ensemble of membrane-bound cytochrome p450 1a1 and cytochrome p450 oxidoreductase. *Communications Biology*, *4*, 1–13, https://doi.org/10.1038/s42003-020-01568-y

Murataliev, M.B., Feyereisen, R., Walker, F.A. (2004). Electron transfer by diflavin reductases. *Archives of Biochemistry and Biophysics*, *1698*, ,

Musumeci, M.A., Botti, H., Buschiazzo, A., Ceccarelli, E.A. (2011). Swapping fad binding motifs between plastidic and bacterial ferredoxin-nadp(h) reductases. *Biochemistry*, *50*, 2111–2122, https://doi.org/10.1021/bi101772a

Nair, D., & Crane, B.R. (2026). Structure and dynamics of a multidomain nitric oxide synthase regulated by a c2 domain. *Science Advances*, *12*, , https://doi.org/10.1126/sciadv.aeb4529

Nakayama, T., Takahashi, S., Waki, T. (2019). Formation of flavonoid metabolons: Functional significance of protein-protein interactions and impact on flavonoid chemodiversity. *Frontiers in Plant Science*, *10*, 821, https://doi.org/10.3389/fpls.2019.00821

Nelson, D., & Werck-Reichhart, D. (2011). A p450-centric view of plant evolution. *The Plant Journal*, *66*, 194–211, https://doi.org/10.1111/j.1365-313X.2011.04529.x

Neunzig, I., Widjaja, M., Peters, F.T., Maurer, H.H., Hehn, A., Bourgaud, F., Bureik, M. (2013). Coexpression of cpr from various origins enhances biotransformation activity of human cyps in S. pombe. *Applied Biochemistry and Biotechnology*, *170*, 1751–1766, https://doi.org/10.1007/s12010-013-0303-2

Nicotra, A.B., Atkin, O.K., Bonser, S.P., Davidson, A.M., Finnegan, E.J., Mathesius, U., et al. (2010). Plant phenotypic plasticity in a changing climate. , *15*, ,

Niu, G., Zhao, S., Wang, L., Dong, W., Liu, L., He, Y. (2017). Structure of the Arabidopsis thaliana nadph-cytochrome p450 reductase 2 (atr2) provides insight into its function. *FEBS Journal*, *284*, 754–765, https://doi.org/10.1111/febs.14017

Ohta, D., & Mizutani, M. (2004). Redundancy or flexibility: Molecular diversity of the electron transfer components for p450 monooxygenases in higher plants. *Frontiers in Bioscience*, *9*, 1587–1597,

Paddon, C.J., & Keasling, J.D. (2014). Semi-synthetic artemisinin: A model for the use of synthetic biology in pharmaceutical development. *Nature Reviews Microbiology*, *12*, 355–367, https://doi.org/10.1038/nrmicro3240

Parage, C., Foureau, E., Kellner, F., Burlat, V., Mahroug, S., Lanoue, A., et al. (2016). Class ii cytochrome p450 reductase governs the biosynthesis of alkaloids. *Plant Physiology*, *172*, 1563–1577, https://doi.org/10.1104/PP.16.00801

Park, S., Kim, Y.S., Rupasinghe, S.G., Schuler, M.A., Back, K. (2013). Rice p450 reductases differentially affect p450-mediated metabolism in bacterial expression systems. *Bioprocess and Biosystems Engineering*, *36*, 325–331, https://doi.org/10.1007/s00449-012-0787-0

Pastorczyk, M., Kosaka, A., Piślewska-Bednarek, M., López, G., Frerigmann, H., Kulak, K., et al. (2020). The role of cyp71a12 monooxygenase in pathogen-triggered tryptophan metabolism and Arabidopsis immunity. *New Phytologist*, *225*, 400–412, https://doi.org/10.1111/nph.16118

Ponnamperuma, K., & Croteau, R. (1996). Purification and characterization of an nadph-cytochrome p450 (cytochrome c) reductase from spearmint (Mentha spicata) glandular trichomes. *Archives of Biochemistry and Biophysics*, *329*, 9–16,

Porter, T.D., Beck, T.W., Kasper, C.B. (1990). Nadph-cytochrome p-450 oxidoreductase gene organization correlates with structural domains of the protein. *Biochemistry*, *29*, 9814–9818,

Porter, T.D., & Kasper, C.B. (1985). Coding nucleotide sequence of rat nadph-cytochrome p-450 oxidoreductase cdna and identification of flavin-binding domains. *Proceedings of the National Academy of Sciences of the United States of America*, *82*, 973–977,

Ralston, L., & Yu, O. (2006). Metabolons involving plant cytochrome p450s. , *5*, ,

Rana, S., Lattoo, S.K., Dhar, N., Razdan, S., Bhat, W.W., Dhar, R.S., Vishwakarma, R. (2013). Nadph-cytochrome p450 reductase: Molecular cloning and functional characterization of two paralogs from Withania somnifera (l.) dunal. *PLoS ONE*, *8*, e57068, https://doi.org/10.1371/journal.pone.0057068

Ro, D.K., Ehlting, J., Douglas, C.J. (2002). Cloning, functional expression, and subcellular localization of multiple nadph-cytochrome p450 reductases from hybrid poplar. *Plant Physiology*, *130*, 1837–1851, https://doi.org/10.1104/pp.008011

Ro, D.K., Ouellet, M., Paradise, E.M., Burd, H., Eng, D., Paddon, C.J., et al. (2008). Induction of multiple pleiotropic drug resistance genes in yeast engineered to produce an increased level of antimalarial drug precursor, artemisinic acid. *BMC Biotechnology*, *8*, 83, https://doi.org/10.1186/1472-6750-8-83

Rosco, A., Pauli, H.H., Priesner, W., Kutchan, T.M. (1997). Cloning and heterologous expression of nadph-cytochrome p450 reductases from the Papaveraceae. *Archives of Biochemistry and Biophysics*, *348*, 369–377, https://doi.org/10.1006/abbi.1997.0374

Ruan, H., Gao, L., Fang, Z., Lei, T., Xing, D., Ding, Y., et al. (2024). A flavonoid metabolon: Cytochrome b5 enhances b-ring trihydroxylated flavan-3-ols synthesis in tea plants. *The Plant Journal*, *118*, 1793–1814, https://doi.org/10.1111/tpj.16710

Sagwan-Barkdoll, L., & Anterola, A.M. (2018). Taxadiene-5α-ol is a minor product of cyp725a4 when expressed in Escherichia coli. *Biotechnology and Applied Biochemistry*, *65*, 294–305, https://doi.org/10.1002/bab.1606

Shephard, E.A., Phillips, I.R., Bayney, R.M., Pike, S.F., Rabin, B.R. (1983). Quantification of nadph:cytochrome p-450 reductase in liver microsomes by a specific radioimmunoassay technique. *Biochemical Journal*, *211*, 333–340,

Simmons, D.L., Lalley, P.A., Kasper, C.B. (1965). Chromosomal assignments of genes coding for components of the mixed-function oxidase system in mice. *Journal of Biological Chemistry*, *260*, 515–521,

Sintupachee, S., Promden, W., Ngamrojanavanich, N., Sitthithaworn, W., De-Eknamkul, W. (2015). Functional expression of a putative geraniol 8-hydroxylase by reconstitution of bacterially expressed plant cyp76f45 and nadph-cytochrome p450 reductase cpr i from Croton stellatopilosus ohba. *Phytochemistry*, *118*, 204–215, https://doi.org/10.1016/j.phytochem.2015.08.005

Spivak, S.G., Berdichevets, I.N., Yarmolinsky, D.G., Maneshina, T.V., Shpakovski, G.V., Kartel, N.A. (2009). Construction and characteristics of transgenic tobacco Nicotiana tabacum l. plants expressing CYP11A1 cdna encoding cytochrome p450scc. *Russian Journal of Genetics*, *45*, 1067–1073, https://doi.org/10.1134/S1022795409090075

Strohmaier, S.J., Huang, W., Baek, J.-M., Hunter, D.J.B., Gillam, E.M.J., Gillam, C.E.M.J. (2019). Rational evolution of the cofactor-binding site of cytochrome p450 reductase yields variants with increased activity towards specific cytochrome p450 enzymes. *FEBS Journal*, *286*, 4473–4493, https://doi.org/10.1111/febs.14982

Su, P., Guan, H., Zhang, Y., Wang, X., Gao, L., Zhao, Y., et al. (2017). Probing the single key amino acid responsible for the novel catalytic function of ent-kaurene oxidase supported by nadph-cytochrome p450 reductases in Tripterygium wilfordii. *Frontiers in Plant Science*, *8*, 1756, https://doi.org/10.3389/fpls.2017.01756

Tan, W., Liao, T.H., Wang, J., Ye, Y., Wei, Y.C., Zhou, H.K., et al. (2020). A recently evolved diflavin-containing monomeric nitrate reductase is responsible for highly efficient bacterial nitrate assimilation. *Journal of Biological Chemistry*, *295*, 5051–5066, https://doi.org/10.1074/jbc.RA120.012859

Tavolieri, A.M., Murray, D.T., Askenasy, I., Pennington, J.M., McGarry, L., Stanley, C.B., Stroupe, M.E. (2019). Nadph-dependent sulfite reductase flavoprotein adopts an extended conformation unique to this diflavin reductase. *Journal of Structural Biology*, *205*, 170–179, https://doi.org/10.1016/j.jsb.2019.01.001

Teoh, K.H., Polichuk, D.R., Reed, D.W., Nowak, G., Covello, P.S. (2006). Artemisia annua l. (asteraceae) trichome-specific cdnas reveal CYP71AV1, a cytochrome p450 with a key role in the biosynthesis of the antimalarial sesquiterpene lactone artemisinin. *FEBS Letters*, *580*, 1411–1416, https://doi.org/10.1016/j.febslet.2006.01.065

Tiedge, K.J., Roda, F., Smith, S.D., Moghe, G.D. (2025). Advances in analyzing and engineering plant metabolic diversity. *Applications in Plant Sciences*, *13*, e70017, https://doi.org/10.1002/aps3.70017

Udhane, S.S., Parween, S., Kagawa, N., Pandey, A.V. (2017). Altered CYP19A1 and CYP3A4 activities due to mutations a115v, t142a, q153r and p284l in human p450 oxidoreductase. *Frontiers in Pharmacology*, *8*, 580, https://doi.org/10.3389/fphar.2017.00580

Ullrich, V. (1979). Cytochrome p450 and biological hydroxylation reactions. (pp. 68–100). University of Saarland.

Urban, P., Mignotte, C., Delorme, R., Pompon, D. (1997). Cloning, yeast expression, and characterization of the coupling of two distantly related Arabidopsis thaliana nadph-cytochrome p450 reductases with p450 CYP73A5. *Journal of Biological Chemistry*, *272*, 19176–19182, https://doi.org/10.1074/jbc.272.31.19176

Van Den Brink, H.J.M., Van Zeijl, C.M.J., Brons, J.F., Van Den Hondel, C.A.M.J.J., Van Gorcom, R.F.M. (1995). Cloning and characterization of the NADPH cytochrome P450 oxidoreductase gene from the filamentous fungus Aspergillus niger. *DNA and Cell Biology*, *14*(8), 719–729, https://doi.org/10.1089/DNA.1995.14.719

Varadarajan, J., Guilleminot, J., Saint-Jore-Dupas, C., Piégu, B., Chabouté, M.E., Gomord, V., et al. (2010). AtR3 encodes a diflavin reductase essential for Arabidopsis embryo development. *New Phytologist*, *187*, 67–82, https://doi.org/10.1111/j.1469-8137.2010.03254.x

Waheed Bhat, W., Rana, S., Dhar, N., Razdan, S., Pandith, S.A., Vishwakarma, R., Lattoo, S.K. (2014). An inducible NADPH-cytochrome P450 reductase from Picrorhiza kurrooa-an imperative redox partner of cytochrome P450 enzymes. *Functional and Integrative Genomics*, *14*, 381–399, https://doi.org/10.1007/s10142-014-0362-7

Walters Biggs, B.W., Lim, C.G., Sagliani, K., Shankar, S., Stephanopoulos, G., De Mey, M., Ajikumar, P.K. (2016). Overcoming heterologous protein interdependency to optimize P450-mediated taxol precursor synthesis in Escherichia coli. *Proceedings of the National Academy of Sciences of the United States of America*, *113*(12), 3209–3214, https://doi.org/10.1073/pnas.1515826113

Wang, M., Roberts, D.L., Paschke, R., Shea, T.M., Masters, B.S.S., Kim, J.-J.P. (1997). Three-dimensional structure of nadph-cytochrome p450 reductase: Prototype for fmn- and fad-containing enzymes. *Proceedings of the National Academy of Sciences of the United States of America*, *94*, 8411–8416,

Warman, A.J., Roitel, O., Neeli, R., Girvan, H.M., Seward, H.E., Murray, S.A., et al. (2005). Flavocytochrome p450 bm3: An update on structure and mechanism of a biotechnologically important enzyme. *Biochemical Society Transactions*, *33*, 747–753, https://doi.org/10.1042/BST0330747

Waskell, L., & Kim, J.-J.P. (2015). Electron transfer partners of cytochrome p450. *Cytochrome p450: Structure, mechanism, and biochemistry* (4th ed., pp. 33–68).

Springer.

Werck-Reichhart, D., Nelson, D.R., Renault, H. (2024). Cytochromes p450 evolution in the plant terrestrialization context. *Philosophical Transactions of the Royal Society B: Biological Sciences*, *379*, , https://doi.org/10.1098/rstb.2023.0363

Whitelaw, D.A., Tonkin, R., Meints, C.E., Wolthers, K.R. (2015). Kinetic analysis of electron flux in cytochrome p450 reductases reveals differences in rate determining steps in plant and mammalian enzymes. *Archives of Biochemistry and Biophysics*, *584*, 107–115, https://doi.org/10.1016/j.abb.2015.09.002

Wolthers, K.R., Lou, X., Toogood, H.S., Leys, D., Scrutton, N.S. (2007). Mechanism of coenzyme binding to human methionine synthase reductase revealed through the crystal structure of the fnr-like module and isothermal titration calorimetry. *Biochemistry*, *46*, 11833–11844, https://doi.org/10.1021/bi701209p

Xia, C., Panda, S.P., Marohnic, C.C., Martásek, P., Masters, B.S.S., Kim, J.-J.P. (2011). Structural basis for human nadph-cytochrome p450 oxidoreductase deficiency. *Proceedings of the National Academy of Sciences of the United States of America*, *108*, 13486–13491, https://doi.org/10.1073/pnas.1106760108

Xia, C., Rwere, F., Im, S., Shen, A.L., Waskell, L., Kim, J.-J.P. (2018). Structural and kinetic studies of asp632 mutants and fully reduced nadph-cytochrome p450 reductase define the role of asp632 loop dynamics in the control of nadph binding and hydride transfer. *Biochemistry*, *57*, 4997–5008, https://doi.org/10.1021/acs.biochem.7b01102

Xia, S., & Hirao, H. (2024). The dissociation process of $nadp^+$ from nadph-cytochrome p450 reductase studied by molecular dynamics simulation. *The Journal of Physical Chemistry B*, *128*, 7159–7168, https://doi.org/10.1021/acs.jpcb.4c03329

Xia, S., & Hirao, H. (2025). Recent advances in elucidating the mechanism of the nadph-cytochrome p450 reductase-mediated electron transfer cycle: Experimental and computational perspectives. *Molecules*, *30*, , https://doi.org/10.3390/molecules30183733

Xie, D.Y., Ma, D.M., Judd, R., Jones, A.L. (2016). Artemisinin biosynthesis in Artemisia annua and metabolic engineering: Questions, challenges, and perspectives. *Phytochemistry Reviews*, *15*, 1093–1114, https://doi.org/10.1007/

s11101-016-9480-2

Zhang, B., Munske, G.R., Timokhin, V.I., Ralph, J., Davydov, D.R., Vermeris, W., et al. (2022). Functional and structural insight into the flexibility of cytochrome p450 reductases from Sorghum bicolor and its implications for lignin composition. *Journal of Biological Chemistry*, *298*, 101761, https://doi.org/10.1016/j.jbc.2022.101761

Zhang, H., Im, S.C., Waskell, L. (2007). Cytochrome b5 increases the rate of product formation by cytochrome P450 2b4 and competes with cytochrome P450 reductase for a binding site on cytochrome P450 2b4. *Journal of Biological Chemistry*, *282*, 29766–29776, https://doi.org/10.1074/jbc.M703845200

Zhang, Y., & Fernie, A.R. (2021). Metabolons, enzyme–enzyme assemblies that mediate substrate channeling, and their roles in plant metabolism. *Plant Communications*, *2*, 100081, https://doi.org/10.1016/j.xplc.2020.100081

Zhao, Q., Smith, G., Modi, S., Paine, M., Wolf, C.R., David, T., et al. (1996). Crystallization and preliminary x-ray diffraction studies of human cytochrome P450 reductase. *Journal of Structural Biology*, *116*, 320–325, https://doi.org/10.1006/jsbi.1996.0048

Zhao, X., Zhao, Y., Gou, M., Liu, C.J. (2023). Tissue-preferential recruitment of electron transfer chains for cytochrome P450-catalyzed phenolic biosynthesis. *Science Advances*, *9*, , https://doi.org/10.1126/sciadv.ade4389

Zhou, A., Zhou, K., Li, Y. (2021). Rational design strategies for functional reconstitution of plant cytochrome P450s in microbial systems. *Current Opinion in Plant Biology*, *60*, 102005, https://doi.org/10.1016/j.pbi.2021.102005